Response to comments on 'A chironomid-based mean July temperature inference model from the south-east margin of the Tibetan Plateau, China'

Editor's comments:
Both reviewers raised the point of removing the 47-lake model. I suggest the authors to consider the use of the larger calibration set alone for the revised version. This would greatly simplify the discussion and avoid potential confusion.

Response: We thank the editor for this comment as well and we revised our manuscript by removing the 47-lake model.

Reviewer 1's comments:

We thank the reviewer for the helpful review and very constructive suggestions. We revised our manuscript by taking into account of virtually all the recommendations. In response to the general point – we removed the 47-lake model from this paper. The original idea by including a 47-lake subset was to compare the performance and the reconstruction results on the same site by applying a local vs. regional transfer functions. However, we agreed that the readability of the paper has improved after we focussed only on the large calibration set. We therefore made this change. This also addressed one of the general comments raised by Reviewer 2.

Specific comments
Line 97. It would be useful to provide references to papers which suggest that reduced local models may be more effective in reconstructions than large models encompassing long temperature gradients (e.g. Velle et al 2011 Holocene).
Response: Comment doesn't apply any more after we removed the 47 dataset.

Line 140. It is important that the authors also quote the present day MJT (rather than MAT) of Tincai Lake since MJT is what they are reconstructing.
Response: we added the value of MJT of Tiancai Lake in this sentence (**Line 151**).

Line 198. The correct reference here is Wiederholm 1983 Ent Scand Suppl. (not Wiederholm 1984).
Response: we corrected this reference accordingly (**Line 209 and Line 951-952**).

Line 205 and elsewhere. Insert 'and abundance' as it is the influence on chironomid abundance as well as distribution that is determined by these numerical methods.
Response: we corrected this accordingly.

Line 206. Table 1 includes 18 variables not 15 as stated in the text.
Response: we corrected this accordingly.

Line 233. It would be useful to plot a PCA of all 18 variables, before elimination of variables

following forward selection, so we can easily assess which variables co-vary and which variables might be influencing chironomid distribution and abundance (see Juggins, 2013).
Response: we agreed with this comment, by also taking into account of Reviewer 2's comment, we added 'we used stepwise selection based on pseudo-F to aid the variable selection process' (**Line 236-237**) instead. This served the same purpose as plotting a PCA of all variables.

Line 304. These taxa may have more cosmopolitan distributions than other taxa in the dataset but they nevertheless must have estimated temperature optima that are used in the model so it would be useful if they were quoted. I would suggest adding the estimated temperature optima after the taxon names in Fig 2. The taxa can then be ranked in that figure left to right in ascending estimated temperature optima.
Response: we modified **Figure 2** by ranking the taxa along the mean July temperature gradient.

Lines 311-320. I am concerned at the large proportion of lotic taxa in this training set which may have poorly estimated temperature optima. The authors do comment on this potential problem however.
Response: we acknowledged this issue and we highlighted this by adding a statement in **Line 456-458**.

Fig 3a and Fig 3c are hard to interpret because the authors do not tell us to which species the code numbers refer. These code numbers either should be explained in the figure caption or preferably should be added after the species names in Fig 2.
Response: We added the species code after the species names in **Fig 2**.

Line 337 and Line 369. Table 2a, 2b and Fig 3a, 3b do not show these correlation results
Response: Table 2a and 2b shows the correlation significance discussed in the respective sentences based on the t-values. We clarified that the significance of each of the correlation is determined based on the t-values (**Line 389**).

Line 413, 414. What are RMSEP s1 + s2 and RMSE s1 and RMSE s2?
Response: we deleted s1+s2 and RMSE s1 and RMSE s2 here and only presented the RMSEP as the standard approach.

Lines 446-459. The problems in modelling modern precipitation and temperature for the calibration set may explain the relatively poor performance of the inference model.
Response: we agree that this is potentially one of the reasons. We added a statement about this in **line 496-498**.

Line 534. All chironomids are benthic, in fact T. gracilentus is sometimes found in temperate shallow eutrophic ponds.
Response: we added this statement in **line 522-524**.

Line 550 and 568. Juggins (2013) argues that the CCA λ1 : λ2 ratio, when Axis 1 is constrained against the variable of interest, should be greater than 1.0 if the variable is to be modelled reliably. In your 100-lake model the ratio is only 0.47. This reflects the fact that MJT is not the main driver of chironomid distribution and abundance in your model. This point needs to be stated as one of the caveats you list from line 569.
Response: We noted that the CCA λ1 : λ2 ratio in most of the training sets in the mid-latitudes and the Southern Hemisphere (e.g. Rees et al., 2008; Chang et al., 2015) is less than 1 this is because minimising other environmental gradients and only extracting the temperature gradient is difficult to achieve when we are away from the NH high latitudes.

Line 586. Why is it important that the RMSEP is around 15% of the total temperature gradient covered by the calibration set? Comparing the new Chinese inference models with other chironomid-based inference models that also have relatively low r2 does not mean that the Chinese model has an acceptable performance. You should also compare the performance of the Chinese model with the chironomid-based inference models of Heiri et al (2011) and Barley et al (2006) that you refer to earlier.
Response: The argument here is now significantly simplified due to the removal of the 47 dataset. In the revised version, we only compared and discussed the RMSEP of the temperature gradient scalar length of our 100-lake dataset with other large datasets worldwide including Heiri et al (2011) (**Line 656-658**).

Line 605. I could not immediately find the results showing the statistical correlation between the inferred records and the instrumental record. In fact this result is presented in the discussion at line 648. It should be moved to the results section.
Response: we moved the statistic P value up in the end of the result section (**Line 475-476**) instead of the discussion.

Line 608 and Fig. 6b. You do not discuss what might be driving the poor fit to temperature of the most recent fossil samples. This result suggests a variable other than temperature might be influencing the chironomids in the most recent period of your sequence. I think it would be informative to plot the fossil samples passively in CCA space of the calibration set to see which environmental variables the taxa were responding to.
Response: We addressed this point by acknowledging that it is possible a second gradient other than mean July temperatures influencing the chironomid species distribution and abundance in most recent fossil samples of Tiancai Lake (**Line 676-679**). These may be related to the human activities i.e. tourist attractions at the site since the recent decade.

Lines 612-615. This sentence should be deleted. It describes methods.
Response: we deleted this sentence (**Line 671 – 674**).

Line 621. Although you adjusted the MJT from Lijiang for altitudinal lapse rate you do not present these results. Instead you plot deviation from the mean in order to compare your results. This shows a close similarity in trends but it would be of interest to see whether the chironomid-inferred temperature estimates were similar to the instrumental records

adjusted for altitude. This would be another useful test of model performance.
Response: We added the plot of the lapse rate corrected mean July temperature curve in **Figure 6a** along with the chironomid-based transfer function reconstructed temperatures.

Line 630. The 47-lake and 100-lake inferred temperature estimates are similar, especially in the most recent part of the record. However the gap between the estimates is greater at the beginning of the record than at the end. Do you have any thoughts on what might be the explanation for this difference?
Response: We removed the plot for the 47-lake based results. A possibility for the gap between the estimates is greater at the beginning of the record is that the larger training set covered a few more sites between 10-12 °C and this may have elevated the curve slightly at relatively warmer period while the 47-lake based results are more flattened.

Line 631 and Fig 6e. It is not apparent from the plot in Fig 6e that the cool and warm periods are amplified by the 100-lake model in comparison with the 47-lake model.
Response: The comment doesn't apply anymore because we removed the plot based on the 47-lake model and focus only on the larger data set so this comment does not apply for the revised version.

Line 632. While I agree that the trends in the instrumental record are well-reflected by the chironomid-inferred record it would also be useful to compare the chironomid-inferred estimates with the lapse rate adjusted instrumental data.
Response: we added the plot of the lapse rate corrected mean July temperature reconstructed using the chironomid transfer function in **Figure 6a**.

Lines 633-638. I could not understand the meaning of these sentences.
Response: These sentences are now simplified due to the removal the 47-lake model related discussion. We now only presented and discussed the 100-lake model reconstructed results and compare with the instrumental record (**Line 708-713**).

Line 648. Results should not be presented in the discussion.
Response: we deleted these sentences (**Line 702-705**).

Line 650. The authors' conclusion that the 100-lake model performs better than the 47-lake model makes me conclude that there is no point in presenting the results of the 47-lake model. I think reference to the smaller model should be deleted from the paper. This would make the paper shorter and easier to follow.
Response: we agreed with this comment and we modified our manuscript by removing the discussion on the 47-lake model.

Conclusion. There is no need to present the performance statistic results again in the conclusion.
Response: we removed the performance of statistics from the conclusion (**Line 738-745**).

Fig 1 caption. Insert '(b)' after '(square box)'. Delete'(b)' and replace with '(c)'
Response: we updated **Figure 1 caption** accordingly (**Line 1001-1005**).

Fig 2a caption. Why are only a few taxa grouped by their thermal preferences? How did you decide that some were better temperature indicators than others? What do you mean by 'optical observation'? The lakes should be listed in descending order of altitude or MJT. This needs to be stated in the caption. I don't understand how T. gracilentus and M. radialis can both be cold indicators when between them they appear to be found in complementary lakes. The estimated temperature optimum of each taxon should be presented after its name in the figure. The CCA sample score is not informative in terms of ranking the taxa when MJT is not the main driver of the taxon distribution and abundance. It would be more useful to rank them by order of temperature optimum. The code number of each taxon used in Fig 3 should also appear next the taxon name in this figure too.
Response: we corrected **Figure 2** by taking both reviewers' suggestions and revised the caption (**line 1007-1014**).

Table 3. The caption is difficult to understand. I suggest replacing the word 'retained' with 'maintained' as I think this would better reflects the results.
Response: we corrected this accordingly in the revised **Table 3 caption (line 1081-1087)**.

Table 4. The results should be quoted to two-decimal places.
Response: we corrected these accordingly in **Table 4**.

<u>Reviewer 2's Comments:</u>

We thank the reviewer for the very useful and constructive review overall, we have considered all the suggestions in our revised version of the manuscript. The reviewer made two general points and in response to the first point, we agreed that we were not explicit about the rationale for using both the 47 and 100 lake calibration sets. We agreed that the paper would be simplified and more concise if we focus only on the large calibration set. We therefore modified our manuscript by removing the sections related to the 47-lakes calibration set.

The second general point mentioned by the reviewer is that the correlation between the instrumental data and the reconstruction may be overstated because of the lack of independence between samples due to autocorrelation. We agree with this point of view however we compared the transfer function model reconstructed results with the instrumental record as an additional diagnostic method because these instrumental data are available from the closest weather station. Before this, we had already applied the 'standard diagnostics' such as goodness-of-fit, modern analogues etc., which all suggested that the results are reliable. These validation methods are relatively independent. The well-compared result with the instrumental record is reassuring that the model is capable to reconstruct the long-term temperature trend that is realistic. We acknowledged this point in the revised manuscript (**Line 725-728**).

###Minor points

Line 183 Böhner 2004 is not in the reference list. It is probably worth clarifying that Böhner uses reanalysis data.

Response: we added Bohner 1994 (instead of 2004) (**Line 798-799**) in the reference listed and clarified that Bohner used reanlaysis data (**Line 195**).

A histogram showing the distribution of lakes along the temperature gradient should be given, or at least discussed, as WAPLS is sensitive to an uneven distribution of lakes.

Response: we highlighted in the discussion about the lake distribution is even along the temperature gradient (**Line 661**).

Line 217 If N (number of lakes) is less than two, Hill's N2 is guaranteed to be less than two.

Response: we corrected this throughout in the revised version (**Line 229**).

Line 223. Variance inflation factors are useful for diagnosing multi-collinearity amongst the predictors, but is less useful for identifying which variable should be deleted. Simply deleting the variable with the highest VIF is a poor strategy. Stepwise selection based on pseudo-F is probably better.

Response: we clarified that we used VIF as one of the methods when considering removing variables in the CCA and we also considered the stepwise selection based on pseudo-F while we were selecting the variables to be included in the CCA (**Line 236-237**).

Line 250. A 2-component WAPLS model is selected although the improvement in model performance is only about 1%, less than the 5% threshold reported. A randomisation t-test is probably a better test than a simple threshold.

Response: taking the reviewer's suggestion, we ran a randomisation t-test to check if component 2 is outperformed much more when comparing to component 1. We found that there is a difference in the RMSEPs between the component 1 and component 2 and we re-affirm that the choice of using WA-PLS component 2 for the reconstruction would give more robust results. We provided this information in **Line 264-266** and **Table 4b** respectively.

Line 296. I think it would be better to show that temperature is an important predictor with the ordination before discussing species temperature preferences.

Response: in the revised version, we stated that temperature is an important predictor before the discussion on the chironomid species and temperature relationship (**Line 312-313**).

Line 309. Move the section on Lake Tiancai chironomids to after transfer function development.

Response: we moved this section accordingly, new **lines 447-458**.

Line 398. It is expected that weighted-averaging with inverse deshrinking and weighted averaging partial least squares component-one will give similar models. Under certain

circumstances, they will be identical.
Response: we pointed this out (**Line 419**).

Line 401. Please don't use novel abbreviations. The space they save is not worth the cognitive load on the reader. No need to report all the performance statistics that are in table 4.
Response: we reduced the use of abbreviations where necessary. In the revised version, we only present the important performance statistics (i.e. only those have discussed/mentioned in the text) in **Table 4**.

Line 438. Please provide a statistical comparison of the reconstruction and the instrumental data. Reporting that they have a "comparable trend" is not sufficient - don't leave it to the discussion to give the correlation.
Response: we moved the statistical p value up to this line instead of leaving it to the discussion (**line 475**).

Line 621. The text suggests that the instrumental data are lapse-rate corrected, whereas the figure suggests that anomalies are compared. Obviously, the former test is much more powerful.
Response: We added the plot of the lapse-rate corrected curve of the chironomid-inferred mean July temperatures in **Fig 6e** along with the plot of the temperature anomalies.

Figure 2 is impossible to interpret as the reader does not know the lake numbers. Sorting the lakes by temperature (and including this information), would make this figure much better.
Response: we modified **Figure 2** by sorting the lakes by mean July temperatures.

Table 3 is rather large and needs to be condensed by extracting just the most important parts (eg L1/L2 for temperature).
Response: we condensed **Table 3**. This table is greatly simplified after we removed the results for the 47 calibration set.

Table 4 needs proper headers, not simply the output from C2.
Response: we modified the caption (**line 1089-1098**) and the titles for **Table 4** to provide a clearer description of the data presented in the table.

The authors should state where the data will be archived.
Response: Our data will be available from State Key Laboratory of Lake Science and Environment webpage in the future.

A chironomid-based mean July temperature inference model from the south-east margin of the Tibetan Plateau, China

Enlou Zhang[a*], Jie Chang[a],Yanmin Cao[b], Hongqu Tang[c], Pete Langdon[d], James Shulmeister[e], Rong Wang[a], Xiangdong Yang[a], Ji Shen[a]

[a] State Key Laboratory of Lake Science and Environment, Nanjing Institute of Geography and Limnology, Chinese Academy of Science, Nanjing 210008, China

[b] College of Resources and Environmental Science, South-Central University for Nationalities, Wuhan 430074, P. R. China

[c] Research Centre of Hydrobiology, Jinan University, Guangzhou 510632, P. R. China

[d] Geography and Environment, University of Southampton, Southampton SO17 1BJ, UK

[e] School of Geography, Planning and Environmental Management, The University of Queensland, St Lucia, Brisbane, Qld 4072, Australia

*Corresponding author Email: elzhang@niglas.ac.cn

Abstract: Chironomid-~~–~~based calibration training set~~s~~ comprised of 100 lakes from south-western China ~~and a subset of 47 lakes from Yunnan Province were~~was established. Multivariate ordination analyses were used to investigate the relationship between the distribution and abundance of chironomid species and 18~~5~~ environmental variables from these lakes. Canonical correspondence analyses (CCAs) and partial CCAs showed that mean July temperature is ~~the sole independent and significant ($p < 0.05$) variable that explains 16% of the variance in the chironomid data from the 47 Yunnan lakes. Mean July temperature remains~~ one of the independent and significant variables explaining the second largest amount of variance after potassium ions (K^+) in the 100 south-western Chinese lakes. Quantitative transfer functions were created using the chironomid assemblages for this ~~both~~ calibration data set~~s~~. The second~~first~~ component of the weighted average partial least square (WA-PLS) model ~~based on the 47 lakes training set~~ produced a coefficient of determination ($r^2_{\text{bootstrap}\cancel{\text{jack}}}$) of 0.6~~8~~3, maximum bias (bootstrap~~jackknifed~~) of 5.16~~3.15~~ and root mean squared error of prediction (RMSEP) of 2.31~~1.72~~ °C. ~~The two-component WA-PLS model for the 100 lakes training set produced an $r^2_{bootstrap}$ of 0.63, maximum bias (bootstrapped) of 5.16 and RMSEP of 2.31 °C.~~ We applied ~~both transfer functions~~the transfer functions to a 150-year chironomid record from Tiancai Lake (26°38′3.8 N, 99°43′E, 3898 m a.s.l), Yunnan, China to obtain mean July temperature inferences. ~~The reconstructed results based on both models showed remarkable similarity to each other in terms of pattern.~~ We validated these results by applying several reconstruction diagnostics and comparing them to a 50-year instrumental record from the nearest weather station (26°51'29.22"N, 100°14'2.34"E, 2390 m a.s.l). The~~Both~~ transfer function~~s~~ performs well in this comparison. We argue that this 100-lake~~e~~ large training set is ~~also~~ suitable for reconstruction work despite the low explanatory power of mean July temperature~~MJT~~ because it contains a ~~more~~ complete range of modern temperature and environmental data for the chironomid taxa observed and is therefore ~~more~~ robust.

Keywords: Chironomids; Temperature reconstruction; the south-east margin of the

Tibetan Plateau; Transfer function; ~~Calibration data-set~~Quantitative paleoclimate record

1 Introduction

South-western ~~(SW)~~ China is an important region for examining changes in low and mid-latitudes atmospheric circulation in the Northern Hemisphere~~ (NH)~~. It lies at the intersection of the influence of the Northern Hemisphere~~H~~ westerlies and two tropical monsoon systems, namely the Indian Ocean South-west Monsoon (IOSM) and the East Asian Monsoon (EAM) and should be able to inform us about changes in both the latitude and longitude of the influence of these respective systems through time. Reconstructing changes in circulation requires information about several climatic parameters, including past precipitation and temperature. While there are reasonable records of precipitation from this region (e.g. Wang et al., 2001, 2008; Dykoskia et al., 2005; Xiao et al., 2014), there is a paucity of information about temperature changes. In order to understand the extent and intensity of penetration of monsoonal air masses, robust summer temperature estimates are vital as this is the season that the monsoon penetrates south-western~~SW~~ China.

Chironomid larvae are frequently the most abundant insects in freshwater ecosystems (Cranston, 1995) and subfossil chironomids are widely employed for palaeoenvironmental studies due to their sensitivity to environmental changes and ability of the head capsules to preserve well in lake sediments (Walker, 2001). A strong relationship between chironomid species assemblages and mean summer air temperature have been reported from many regions around the world and transfer functions were subsequently developed (e.g. Brooks and Birks, 2001; Larocque et al., 2001; Heiri et al., 2003; Gajewski et al., 2005; Barley et al., 2006; Woodward and Shulmeister, 2006; Langdon et al., 2008; Rees et al., 2008; Eggermont et al., 2010; Luoto, 2009; Holmes et al., 2011; Heiri et al., 2011; Chang et al., 2015a). The application of these transfer functions has provided quantitative temperature data since the last glacial period in many regions of the world (e.g. Woodward and Shulmeister, 2007; Rees and Cwynar, 2010; Samartin et al., 2012; Chang et al., 2015b; Muschitiello et al., 2015; Brooks et al., 2016). Consequently, subfossil chironomids have been the most widely applied proxy for past summer temperature reconstructions.

Merged regional chironomid training sets and combined inference models have been developed in Europe (Lotter et al., 1999; Holmes et al., 2011; Heiri et al., 2011; Luoto et al., 2014). These large datasets and models provide much more robust reconstructions than smaller local temperature inference models (Heiri et al., 2011; Luoto et al., 2014). However, the distribution of large regional inference models is limited to Europe and northern North America (e.g. Fortin et al., 2015). There is a need to build large training sets for other parts of the world where chironomids will likely be sensitive to temperature changes. Subfossil chironomids have been successfully used as paleoenvironmental indicators in China for over a decade. These included salinity studies on the Tibetan Plateau (Zhang et al, 2007) and the development of a nutrient based inference model for eastern China and parts of Yunnan (Zhang et al., 2006, 2010, 2011, 2012). A large database of relatively undisturbed lakes, in which nutrient changes are minimal while temperature gradients are suitably large, is now available from south-~~-~~western China and this provides the opportunity to develop a summer temperature inference model for this broad region.

In this study, a chironomid species assemblage training set and~~ a~~ chironomid-based mean July air temperature ~~(MJT) ~~inference models from 100 lakes on the south-east margin of the Tibetan Plateau are~~is~~ developed. ~~We also present a 47 lake subset of the training set to provide a local model for Yunnan Province. We compare the output of the two models and evaluate which model is more robust and more suitable for temperature reconstructions in Yunnan. Finally, w~~We test and validate ~~both models~~the selected transfer function models by ~~comparing a reconstruction of temperature from~~applying it to a sediment core collected from Tiancai Lake (26°38′3.8 N, 99°43′E, 3898 m a.s.l) (Fig. 1) in Yunnan Province, south-western~~SW~~ China for the last 120 years against a 50-year long~~n~~ instrumental record from Lijiang weather station (26°51'29.22"N, 100°14'2.34"E, 2390 m a.s.l) (Fig. 1), which is the closest meteorological station with the~~a~~ longest record.

2 Regional setting

The study area lies in the south-east margin of the Tibetan Plateau including the south-west part of Qinghai Province, the western part of Sichuan Province and the north-west part of Yunnan Province (Fig. 1). It is situated between 26 – 34° N, 99 – 104° E with elevations ranging from about 1000 m to above 5000 m a.s.l.. ~~. The 47 lake subset is confined to the north-west part of Yunnan province (Fig. 1) and includes the area around Tiancai Lake.~~

The study area is characterized by many north-south aligned high mountain ranges (e.g. Hengduan Mountains, Daxue Mountains, Gongga Mountains etc.) that are fault controlled and fall away rapidly into adjacent tectonic basins. The mountain ranges have been deeply dissected by major rivers including the Nujiang, Lancangjiang, Jinshajiang, Yalongjiang and Dadu rivers. Local relief in many places exceeds 3000 m a.s.l..

The climate of the study area is dominated by the westerlies in winter and by the IOSM in Yunnan and Tibet, but some of the easternmost lakes are affected by the EAM. There is a wet season that extends from May (June) to October accounting for 85-90% of total rainfall and a dry season from November to April. Annual precipitation varies greatly according to altitude and latitude. Most of the precipitation is derived from a strong south-west summer monsoonal flow that emanates from the Bay of Bengal (Fig. 1). Precipitation declines from south-east to north-west. Mean summer temperatures vary between about 6 to 22 °C from the north-west to the south-east (Institute of Geography, Chinese Academy of Sciences, 1990). Vegetation across the study area changes from warm temperate to subtropical rainforest at lower elevations in the south-west to alpine grasslands and herb meadows at high altitude.

2.1 Description of model validation site

Tiancai Lake (26°38′3.8 N, 99°43′E, 3898 m a.s.l) (Fig. 1) is in Yunnan Province, on the south-east margin of the Tibetan Plateau. It is a small alpine lake and has a maximum depth of 7 m, with a water surface area of ~ 2.1 ha and a drainage area of ~3 km^2. Tiancai Lake is dominated in summer by the IOSM, and most likely retains a tropical airflow in winter as the climate is remarkably temperate for this altitude. The mean annual and July air temperatures are~~is~~ approximately 2.5 °C and 8.4 °C respectively, and the annual precipitation is modelled as > 910 mm (Xiao et al. 2014). The lake is charged by 3 streams and directly from precipitation and drains into a lower alpine lake via a stream. The most common rock type in the catchment is a quartz poor granitoid (syenite). Terrestrial vegetation in the catchment consists mainly of conifer forest comprising *Abies* sp. and *Picea* sp. with an understory of *Rhododendron* spp. Above the tree-line, at about 4100 m a.s.l, Ericaceae shrubland (rhododendrons) gives way to alpine herb meadow and rock screes.

3 Methodology

3.1 Field and laboratory analysis

Surface sediment samples were collected from 100 lakes in the south-east margin of the Tibetan Plateau via six field campaigns during the autumn of each year between 2006 and 2012. The lakes in this area are mainly distributed at the top or upper slopes of the mountains and are primarily glacial in origin. Most lakes were reached by hiking or with horses and the lake investigation spanned several seasons. Small lakes (surface area c. ~1 km^2) were the primary target for sampling but some larger lakes were also included.

Surface sediments (0-1 cm) were collected from the deepest point in each lake after a survey of the bathymetry using a portable echo-sounder. Surface sediment samples were taken using a Kajak gravity corer (Renberg, 1991). The samples were stored in plastic bags and kept in the refrigerators at 4 °C before analysis. A 30 cm short core was extracted from the centre of Tiancai Lake at a water depth of 6.8 m using UWITEC gravity corer in 2008. The sediment core was sub-sampled at 0.5 cm contiguous intervals and refrigerated at 4°C prior to analysis.

Water samples were collected for chemical analysis from 0.5 m below the lake surface immediately before the sediment samples were obtained. Water samples for chemical analysis were stored in acid-washed polythene bottles and kept at 4 °C until analyses. Secchi depth was measured using a standard transparency disc. Conductivity, pH and dissolved oxygen (DO) were measured in the field using a HI-214 conductivity meter, Hanna EC-214 pH meter and JPB-607 portable DO meter. Chemical variables for the water samples including total phosphorus (TP), total nitrogen (TN), chlorophyll-*a* (chl *a*), K^+, Na^+, Mg^{2+}, Ca^{2+}, Cl^-, SO_4^{2-}, NO_3^- were determined at the Nanjing Institute of Geography and Limnology, Chinese Academy of Sciences. The surface sediments were also analysed for percentage loss-on-ignition (% LOI) following standard methods (Dean 1974). Site-specific values for the mean July air temperature (MJT) and mean annual precipitation (MAP) were estimated using climate layers that were created using statistical downscaling of General Circulation Model (GCM) outputs and terrain parameterization methods in a regular grid network with a grid-cell spacing of 1 km^2 (Böhner 1994~~2004~~, 2006; Böhner and Lehmkuhl, 2005) using reanalysis data. MJT is used to represent summer temperatures because July is the warmest month in south-western China.

3.2 Chironomid analyses

100 surface sediment samples from lakes of south-western China and 55 sub-samples from the Tiancai Lake short core were analysed for chironomids following standard methods (Brooks et al, 2007). The sediment was deflocculated in 10% potassium hydroxide (KOH) in a water bath at 75 °C for 15 minutes. The samples were then sieved at 212 µm and 90 µm and the residue was examined under a stereo-zoom microscope at x 25. Chironomid head capsules were hand-picked using fine forceps. All the head capsules found were mounted on microscope slides in a solution of Hydromatrix®. Samples produced less than 50 head capsules were not included in the subsequent analyses (Quinlan and Smol, 2001). The chironomid head capsules were identified mainly following Wiederholm (1983~~4~~), Oliver and Roussel (1982), Rieradevall and Brooks (2001), Brooks et al. (2007) and a photographic guide provided in Tang (2006).

3.3 Numerical analysis

A range of numerical methods were used to determine the relative influence of the measured environmental parameters on the distribution and abundance of chironomids in the surface sediments within the training set. A total of eighteen ~~fifteen~~ environmental variables were considered in the initial statistical analyses (Table 1). These measurements were normalized using a $\log_{10}$ transformation prior to ordinations following a normality assessment of each data set. Chironomid species were used in the form of square root transformed percentage data in all statistical analyses. The ordinations were performed using CANOCO version 4.5 (ter Braak and Šmilauer, 2002). A detrended correspondence analysis (DCA; Hill and Gauch, 1980) with detrending by segments and nonlinear rescaling was used to explore the chironomid distribution pattern. The DCA was also used to identify the gradient length within the chironomid data and hence whether unimodal analyses were appropriate (ter Braak, 1987). Canonical correspondence analysis (CCA) down-weighted for rare taxa (with a maximum abundance of less than 2% and/or occurred in fewer than two lakes, i.e. Hill's ~~N < 2,~~ $N_2 < 2$), with forward selection and Monte Carlo permutation tests (999 unrestricted permutations) was then used to identify the statistically significant ($p < 0.05$) variables influencing the chironomid distribution and abundance (ter Braak and Šmilauer, 2002). A preliminary CCA with all eigh~~fif~~teen variables was used to identify redundant variables, reducing excessive co-linearity among variables (Hall and Smol, 1992), i.e. the environmental variable with highest variance inflation factor (VIF) was removed after each CCA and the CCA was repeated until all VIFs were less than 20 (ter Braak and Šmilauer, 2002). In addition, we used stepwise selection based on pseudo-F to aid the variable selection process. Only the remaining significant ($p < 0.05$) variables were included in the final CCA ordination. The relationship between the significant environmental variables and ordination axes was assessed with canonical coefficients and the associated t-values of the environmental variables with the respective axes. CCA bi-plots of sample and species scores were generated using CanoDraw (ter Braak and Šmilauer, 2002). Partial canonical correspondence analyses (pCCAs) were applied to test the direct and indirect effects of each of the significant variables in relation to the chironomid species data. These were performed for each of the significant variable with and without the remaining significant variables included as co-variables. Environmental variables that retained their significance after all pCCAs were selected for use in the analyses as they are the independent variables.

Chironomid-~~-~~based transfer functions were developed for mean July temperatures~~MJT~~ using C2, version 1.5. (Juggins, 2005) ~~. Inference models were developed~~ for the ~~subset of 47 lakes located in Yunnan Province close to or above 4000 m a.s.l. and the full~~ calibration data set comprised of~~of~~ 100 lakes~~, respectively~~. The models were constructed using algorithms based on weighted-averaging (WA) and weighted-averaging partial-least-squares (WA-PLS) (Birks, 1995). ~~Jackknifing was applied for the Yunnan calibration data set of 47 lakes as this technique is more robust for data sets with fewer than 80 sites (Kim and Han, 1997).~~ Bootstrap cross-validation technique was tested for the ~~full calibration dataset of 100 lakes~~ dataset as previously demonstrated that it is more suitable for large datasets (Heiri et al., 2011) comparing to the jackknife technique. Transfer function models were evaluated based on the performance of the coefficient of determination (r^2_{boot}), average bias of predictions, maximum bias of predictions and root mean square error of prediction ($RMSEP_{boot}$). The number of components included in the final model was selected based on reducing the RMSEP by at least 5% (Birks, 1998). In addition, instead of using 5% as a simple threshold we also performed a t-test to further check if the additional component of the WA-PLS model is outperformed.

The transfer function models ~~based on the 100 full calibration data set and the subset of 47 lakes~~ were then applied to the fossil chironomid data from Tiancai Lake~~, respectively~~. Mean July temperatures~~JTs~~ (MJT) were reconstructed from the site and three types of reconstruction diagnostics suggested in Birks (1995) were applied to assess the reliability of the results. These include goodness-of-fit, modern analogue technique (MAT) and the percentage (%) analysis of modern rare taxa in the fossil samples. For the goodness-of-fit analysis, the squared residual length (SqRL) was calculated by passively fitting fossil samples to the CCA ordination axis of the modern training set data constrained to MJT in CANOCO version 4.5 (ter Braak and Smilauer, 2002). Fossil samples with a SqRL to axis 1 higher than the extreme 10 and 5% of all residual distances in the modern calibration dataset were considered to have a 'poor' and 'very poor' fit with MJT respectively. The chi-square distance to the closest modern assemblage data for each fossil sample was calculated in C2 (Juggins, 2005) using the MAT. Fossil samples with a chi-square distance to the closest modern sample larger than the 5th percentile of all chi-square distances in the modern assemblage data were identified as samples with 'no good' analogue. The percentage of rare taxa in the fossil samples was also calculated in C2 (Juggins, 2005), where a rare taxon has a Hill's $N_2 < 2$ in the modern data set (Hill, 1973). Fossil samples that contain > 10% of these rare taxa were likely to be poorly estimated (Brooks and Birks, 2001). Finally, the chironomid-based transfer functions inferred MJT patterns were compared to the instrumental recorded data from Lijiang weather station between the years of 1951 and 2014.

3.4. Chronology for Tiancai Lake core

The top 28 cm of the sediment core recovered from Tiancai Lake were used for ^{210}Pb dating. Sediment samples were dated using ^{210}Pb and ^{137}Cs by non-destructive gamma spectrometry (Appleby and Oldfield, 1992). Samples were counted on an Ortec HPGe GWL series well-type coaxial low background intrinsic germanium detector to determine the activities of ^{210}Pb, ^{226}Ra and ^{137}Cs. A total of 58 samples at an interval of every 0.5 cm were prepared and analysed at the Nanjing Institute of Geography and Limnology, Chinese Academy of Sciences. Sediment chronologies were calculated using a composite model (Appleby, 2001). ^{137}Cs was used to identify the 1963 nuclear weapons peak, which was then used as part of a constant rate of supply (CRS) model to calculate a ^{210}Pb chronology for the core.

4 Results

4.1 Distribution of chironomid taxa along the temperature gradient

A total of ~~53 non-rare taxa (N > 2 and N~~$_2$~~ > 2) (Brooks and Birks, 2001) chironomid taxa were identified from the 47 Yunnan lakes and a total of~~ 8~~9~~5 non-rare taxa (Hill's $N_2 > 2$)

(Brooks and Birks, 2001) were identified from 100 south-western Chinese lakes (Fig. 2a). Only these non-rare taxa were included in the final transfer function models. Mean July temperature is an important variable driving the distribution and abundance of the chironomid taxa in this dataset (Fig. 2a). ~~developed based on the Yunnan subset and full calibration data set respectively.~~ Common cold stenotherms, here defined as taxa with a preference for < 12°C MJT include *Heterotrissocladius marcidus*-type, *Tanytarsus gracilentus*-type, *Paracladius*, *Micropsectra insignilobus*-type, *Micropsectra radialis*-type, *Tanytarsus lugens*-type~~, *Thienemanniella clavicornis*-type~~, *Micropsectra* Type A, *Pseudodiamesa*, *Micropsectra atrofasciata*-type and *Corynoneura lobata*-type (Fig. 2a). Taxa characterizing warmer temperatures (> 12°C) include *Polypedilum nubeculosum*-type, *Eukiefferiella* ~~*gracei*-~~*devonica*-type, *Microtendipes pedellus*-type and *Tanytarsus lactescens*-type and *Chironomus plumosus*-type (Fig. 2a). Many of the remaining taxa reflect more cosmopolitan distributions, these include *Procladius*, ~~*Chironomus anthracinus*-type, *Chironomus plumosus*-type,~~ *Corynoneura scutellata*-type, *Tanytarsus pallidicornis*-type, *Tanytarsus mendax*-type and *Paratanytarsus austriacus*-type (Fig. 2a).

~~4.2 Chironomid taxa in Tiancai Lake~~

~~A total of 55 sub-samples were analysed for chironomid taxa throughout the top 28 cm of the core recovered from Tiancai Lake. There were 41 non-rare ($N > 2$, $N_2 > 2$) taxa present (Fig. 2b). The general assemblages of these 55 sub-samples include *Heterotrissocladius marcidus*-type, *Tvetenia tamafalva*-type, *Micropsectra insignilobus*-type, *Corynoneura lobata*-type, *Paramerina divisa*-type, *Micropsectra radialis*-type, *Paratanytarsus austriacus*-type, *Thienemanniella clavicornis*-type, *Eukiefferiella claripennis*-type, *Rheocricotopus effusus*-type, *Macropelopia*, *Pseudodiamesa* and *Procladius* (Fig. 2b). All the taxa identified from this record were well represented, and most of them were recognized as cold stenotherms, in the modern calibration training sets (Fig. 2a).~~

4.2~~3~~ Ordination analyses and model development

~~Detrended canonical analyses (DCAs) performed on the 47 lakes from Yunnan showed the gradient length of axis 1 was 3.328, indicating a direct unimodal method was appropriate to model the chironomid species response (Birks 1998). CCAs were then performed on the 47 Yunnan lakes, 53 non-rare taxa and 15 environmental variables. The initial CCA showed total dissolved solids (TDS) had the highest VIF and was removed from further analyses. Among the remaining 14 variables, eight explained a significant ($p < 0.05$) proportion of variance in the chironomid species data (Table 2a, Fig. 3a, b). These were MJT (16%), conductivity (10.7%), K^+ (10.7%), Ca^{2+} (9.9%), TP (5.7%), Cl^- (5.5%), depth (4.4%) and LOI (3.7%). A total of 30.2% variance was explained by the first four CCA axes using the eight significant variables with the first CCA axis explaining nearly half of the total variance. Among these variables, MJT, K^+, depth and Ca^{2+} showed a significant correlation ($p < 0.01$) with CCA axis 1 and Cl^-,~~

~~MJT, LOI, Ca^{2+} showed a significant correlation ($p < 0.01$) with CCA axis 2 (Table 2a, Fig. 3a, b). MJT explained the largest amount of variance (16%) in the chironomid species data and showed the strongest correlation with CCA axis 1 (Table 2a). The pCCAs results indicated that within the eight significant variables, only MJT retained its significance ($p < 0.01$) after partialling out using pCCAs (Table 3a).~~

~~A bi-plot of the CCA species scores indicating the percent of variance explained by the CCA axes in each chironomid taxon with respect to the environmental variables (Fig. 3a). *Microtendipes pedellus*-type, *Einfeldia natchitocheae*-type, *Paratanytarsus penicillatus*-type, *Tanytarsus medax*-type, *Chironomus anthracinus*-type, *Cladopelma edwardsi*-type, *Dicrotendipes nervosus*-type, *Ablabesmyia*, *Tanytarsus pallidicornis*-type, *Procladius*, *Chironomus plumosus*-type, *Cricotopus sylvestris*-type, *Polypedilum nubeculosum*-type, *Tanytarsus lactenscens*-type displayed a substantial amount of variance with the first two CCA axes and were positively correlated with CCA axis 1. These taxa were associated with warm temperatures. *Heterotrissocladius marcidus*-type, *Tanytarsus lugens*-type, *Parametriocnemus*, *Eukiefferiella gracei*-type, *Paramerina divisa*-type and *Micropsectra* type A, showed a negative correlation with CCA axis 1 and these taxa were inferred as cold temperature indicators. A bi-plot of the CCA sample scores revealed that a large number of sites are closely distributed around depth and LOI, respectively, despite of the low explanatory power of these two variables in the 47 lakes training set (Fig. 3b).~~

The detrended canonical analyses (DCAs) performed on the ~~full calibration training set of~~ 100 lakes and 8~~9~~5 non-rare chironomid taxa had an axis 1 gradient length of 3.033 indicating a CCA approach was appropriate for modelling the chironomid taxa response (Birks, 1998). The ~~same 15~~eighteen environmental variables were tested as in the initial CCA and the results showed that TDS had the highest VIF. It was then removed from the following CCAs. Seven of the remaining ~~14~~ variables had significant ($p < 0.05$) explanatory power with respect to the chironomid species data. These were K^+ (4.8%), MJT (4.4%), conductivity (4.4%), Cl^- (3.4%), LOI (3.1%), Na^+ (2.7%) and depth (2%) (Table 2~~b~~). A total of 14.6% of variance was explained by the four CCA axes with the seven~~7~~ significant variables included and the first two axes explained 10% of the total variance. Of these variables, conductivity and K^+ were significantly correlated ($p < 0.01$) with CCA axis 1 and cond, depth, Cl^-, MJT showed a significant correlation ($p < 0.01$) with CCA axis 2 (Table 2~~b~~, Fig. 3a, b, based on the t-values). Potassium ions (K^+) explained the largest variance in the chironomid species data and showed the strongest correlation with CCA axis 1. MJT and conductivity explained equally the second largest amount of variance (4.4%) where MJT was significantly correlated with CCA axis 2 and conductivity was significantly correlated with both axis 1 and 2 (Table 2~~b~~). The pCCAs (Table 3~~b~~) demonstrated that within the ~~7~~ significant variables K^+, MJT, Cl^-, LOI and depth remained~~tained~~ their significance ($p < 0.01$) when the other variables were included as co-variables. Potassium ions (K^+) is the independent variable dominates the first CCA axis. MJT and Cl^- are the independent variables dominating the second CCA axis but MJT has an overall higher explanatory power (Table 2~~b~~).

A bi-plot of the CCA species scores indicated that taxa such as *Heterotrissocladius marcidus*-type and *Tanytarsus lugens*-type had a significant amount of variance explained by the first two CCA axes and were negatively correlated with CCA axis 1. Taxa including *Polypedilum nubeculosum*-type, *Chironomus plumosus*-type were positively correlated with CCA axis 1 with a significant amount of variance explained by the CCA axis 1 and 2. A bi-plot of the CCA sample scores showed that a major proportion of sites distributed concentrating around depth (Fig. 3b) whereas depth only explains 2% of the total variance in the chironomid ~~100 lakes calibration~~ data~~set~~.

The transfer functions were developed for mean July temperature (MJT) ~~based on the subset with 47 Yunnan lakes and the full 100 lakes calibration datasets, respectively~~. We acknowledge that MJT is not the sole independent variable on CCA axis 2 in the ~~100 lake~~ dataset but transfer functions based on this large regional dataset are created and applied to reconstruct MJT because it is a more useful parameter compared to K^+ and Cl^- ~~for the purpose of comparing the performance with the more localized Yunnan transfer function models~~. Both weighted averaging (WA) and weighted averaging partial least squares (WA-PLS) models were tested ~~for MJT~~ in the ~~respective~~ modern calibration set~~s~~. Summary statistics of inference models based on these two different numerical methods are listed in Table 4a. As expected, t~~T~~he bootstrapped WA with inverse deshrinking (WAinv) and WA-PLS models generated similar statistical results for the ~~both~~ calibration training set~~s~~. ~~For the subset of 47 Yunnan lakes, the WAinv model produced a strong jackknifed coefficient of determination (r^2_{jack}) of 0.83, average bias (AveBiasjack) of 0.113, maximum bias (MaxBiasjack) of 2.83 and root mean squared error of prediction (RMSEP) of 1.67 °C (Table 4a). The first component of WA-PLS model was selected and it produced the same r^2_{jack} of 0.83, AveBiasjack of 0.109, a slightly higher MaxBiasjack of 3.15 and RMSEP of 1.72 °C (Table 4a). Fig. 4a and 4b show the chironomid-inferred versus observed MJT and the distribution of prediction residuals for the transfer function models based on the subset of 47 lakes from Yunnan.~~

~~For the full calibration set of 100 south-western Chinese lakes, bootstrap cross-validation techniques was applied for both the WAinv and WA-PLS models (Table 4). Similar to the Yunnan subset, the WAinv and WA-PLS model produced comparable statistical results.~~ The WAinv model produced an r^2_{boot} of 0.61, AveBiasboot of 0.06, MaxBiasboot of 5.30 and RMSEP ~~(s1 + s2)~~ of 2.30 °C ~~(RMSEs1 = 0.69 °C and RMSEs2 = 2.19 °C)~~ (Table 4a). We selected the second component of WA-PLS bootstrap model as it is ~~the most~~ more robust according to the t-test results (Table 4b). ~~and reduced the RMSEP by more than 5%.~~ It produced an r^2_{boot} of 0.63, AveBiasboot of 0.101, a lower MaxBiasboot of 5.16 and RMSEP ~~(s1 + s2)~~ of 2.31 °C ~~(RMSEs1 = 0.89 °C and RMSEs2 = 2.14 °C)~~. Figures~~.~~ 4c and 4d show the chironomid-inferred versus observed MJT and the distribution of prediction residuals for the above transfer function models respectively ~~based on the full calibration training~~

~~set of 100 lakes~~.

4.3~~4~~ Reconstructions from Tiancai Lake

A total of 55 sub-samples were analysed for chironomid taxa throughout the top 28 cm of the core recovered from Tiancai Lake. There were 41 non-rare (Hill's N_2 > 2) taxa present (Fig. 2b). The general assemblages of these 55 sub-samples include *Heterotrissocladius marcidus*-type, *Tvetenia tamafalva*-type, *Micropsectra insignilobus*-type, *Corynoneura lobata*-type, *Paramerina divisa*-type, *Micropsectra radialis*-type, *Paratanytarsus austriacus*-type, *Thienemanniella clavicornis*-type, *Eukiefferiella claripennis*-type, *Rheocricotopus effusus*-type, *Macropelopia*, *Pseudodiamesa* and *Procladius* (Fig. 2b). All the taxa identified from this record were well represented, and most of them were recognized as cold stenotherms, in the modern calibration training sets (Fig. 2a). We acknowledge that some of the lotic taxa may result in poor temperature estimates when applying the transfer function therefore, reconstruction diagnostics were necessary.

The ^{210}Pb dating results demonstrated that the top 28 cm of the short core recovered ~~-~~ from Tiancai Lake represent the last c. ~150 years (Fig 5). We applied ~~all four~~both new transfer function models (~~WA-47 lakes,~~ WA and ~~-100 lakes, WAPLS-47 lakes,~~ WA-PLS based on~~-~~100 lakes) to reconstruct the MJT changes between 1860 AD and 2008 (Fig. 6a). The WA and WA-PLS models constructed ~~based on the subset of Yunnan lakes and the full calibration dataset 100 lakes~~ showed identical trends in the MJT reconstructions over the last c. ~150 years (Fig. 6a). There were small deviations in terms of absolute values but the variations in the reconstructed MJT ~~among the four~~between the two models were within 0.1~~-0.5~~ °C for each sample (Fig. 6a). Goodness-of-fit analysis on the reconstruction results ~~based on the 100 lake dataset~~ showed that out of the 55 fossil samples, eight samples from the years between 2000 and 2007 AD have 'poor' and 'very poor' fit to MJT (Fig. 6b). The modern analogue analysis showed that only four fossil samples have 'no good' analogues in the 100 lake dataset (Fig. 6c). All 55 fossil samples contain less than 10% of the taxa that were rare in the modern 100 lake training set (Fig. 6d). Finally, the reconstructed results also showed a comparable MJT trend and a statistical significant correlation ($p < 0.05$, $r = 0.45$, $n = 31$) with the instrumental measured data between 1951 and 2007 AD from Lijiang weather station (Fig. 6e).

5 Discussion

5.1 Reliability of the environmental and chironomid data

Obtaining reliable estimates of the modern climate data has been challenging in south-western China. There are very few meteorological stations and climate monitoring in the high mountains of our study area is virtually non-existent. Climate parameters including mean July temperatures~~MJT~~ and mean annual precipitation used in this study are interpolated from climate surfaces derived from a mathematical climate surface model based on the limited meteorological data and a digital terrain model (DTM) applied to the whole of the wider Tibetan region (4000 x 3000 km) (Böhner, 2006). We acknowledge that there are limitations in these data due to the sparse distribution of observations from meteorological stations. Modelling precipitation in topographically complex parts of this region such as~~ the~~ Yunnan is problematic due to the orographic interception (or non-interception) of monsoonal air masses upwind of the sites, but the scale of the DTM means that mean temperature data should be reasonably robust, except in the most topographically complex areas. Further meteorological observations are required to refine this and other studies.~~.~~ We suspect that this is potentially an issue resulting the relatively low transfer function model coefficient (r^2_{boot}).

We examined the chironomid taxa that appeared as temperature indicators in the ~~in the 47 and ~~calibration ~~100 lake data~~sets~~s respectively~~. A number of taxa, namely *Pseudod~~D~~iamesa*, ~~*Parametriocnemus*~~ *Pseudosmittia* and ~~*Tvetenia tamafalva*~~*Corynoneura lobata*-type emerge as cold stenotherms. ~~in the 47 lake dataset but not in the 100 lake dataset. *Diamesa*, *Parametriocnemus* and *Tvetenia tamafalva*-type displayed a more cosmopolitan distribution in the larger training set. We f~~Further examination of~~ed~~ these taxa ~~and we identified~~show that ~~Diamesa, Parametriocnemus and Tvetenia tamafalva-type~~these three taxa are all likely lotic (Cranston, 2010). These taxa would possibly~~likely~~ have washed in to the lakes from streams and therefore it is not appropriate to make temperature inferences based on them. ~~While they appeared as cold stenotherms in the 47 lakes dataset, it is mainly because this training set had lakes with limited in flows except in the alpine lakes. This created the impression of these taxa being cold stenotherms whereas the inclusion of additional lowland lakes that had stream inflows in the larger data set allowed the identification of this misrepresentation. In summary, the 100 lake training set has allowed better identification of environmental tolerance of chironomid taxa in the south-western China data sets.~~

We also observed that another cold stenotherm *Tanytarsus gracilentus*-type is closely related to lake depth, while both *Tvetenia tamafalva*-type and *Micropsectra* show closer correlation with LOI and Cl^- in the CCA biplot (Fig. 3a). The observations match with the ecological recognition and interpretation of these taxa in literature where *Tanytarsus gracilentus*-type was identified as a benthic species in the arctic and is sometimes found in temperate shallow eutrophic ponds (Einarsson et al., 2004; Ives et al., 2008); *Tvetenia tamafalva*-type was often found in streams and this is likely related to the organic content (LOI) of the substrates as they are detritus feeders (Brennan and McLachlan, 1979); while *Micropsectra* was found in thermal springs and pools (Hayford et al., 1995; Batzer and Boix, 2016) and this is reflected in this dataset with having a close relationship with Cl^-. It presents in lakes such as Lake Tengchongqinghai, Qicai Lake and Lake Haizibian that have high levels of Cl^- ions. These sites are located in geothermal spring region of Sichuan and Yunnan Provinces.

Well-known warm stenotherms that are distributed along the MJT gradient of the CCA species bi-plot (Fig. 3a) include *Dicrotendipes*, *Microchironomus*, *Polypedilum* and *Microtendipes*. Many studies (e.g. Walker et al. 1991; Larocque et al. 2001; Rosenberg et al., 2004; Brodersen and Quinlan, 2006; Woodward and Shulmeister, 2006) show that these taxa are warm temperature indicators worldwide. We therefore argue that this large calibration training set contains a relatively complete range of temperatures and environments expected to have been experienced by lakes and their chironomid fauna in the past (Brooks and Birks, 2001). This will be particularly useful when applying the models to reconstruct changes in the late Pleistocene and Holocene when climates were different (Heiri et al., 2011).

~~5.2 Comparison of environmental gradients between the 47 and 100 lakes datasets~~

~~The training set, comprising 47 lakes in Yunnan covers MJTs between 5.6 °C and 18.8 °C and yields a MJT gradient of 13.2 °C. The ordination analyses (CCAs and pCCAs) of this dataset showed that MJT is the only independent variable on CCA axis 1 and explained the largest amount of the total variance (16%) in the chironomid data. Based on these statistical results, the 47 Yunnan lake training set initially appeared more appropriate for developing a MJT chironomid-based transfer function (Juggins, 2013).~~

This~~e~~ 100-~~-~~lake training set covers a ~~longer~~ temperature gradient ranging from 4.2 °C to 20.8 °C (MJT gradient of 16.6 °C). Based on the CCAs, we observed that the MJT signal in this larger training set is partially masked by a salinity gradient. This is represented by potassium ions (K^+) and conductivity (Fig. 3a~~c~~, b~~d~~). CCA axis 1 is dominated by K^+ and this may be related to weak weathering. This is because (1) the first CCA axis is driven by lakes that have low precipitation but intermediate level of evaporation, examples of these sites include Lake Xiniuhaijiuzhai, Lake Muchenghai and Lake Kashacuo, from the north margin of Sichuan Province. These lakes indicate cool, dry and low windiness conditions that lead to a weak weathering environment. We highlight that this area is different from the high Tibetan Plateau where aridity and salinity dominates. (2) In chemical weathering sequences, K^+ is an early stage weathering product (Meunier and Velde, 2013) and K^+ is often associated with primary minerals, such as feldspars and micas in the bedrock (Hinkley, 1996). Salinity is responding to both temperature and aridity but further pCCAs (Table 3) indicate that both K^+ and MJT are independent variables in this training set.

The second CCA axis is co-dominated by MJT and Cl^- with very similar gradient lengths. Lakes distributed along the warmer end of the MJT gradient include Lake Longtan, Lake Lutu, Lake Luoguopingdahaizi and Lake Jianhu. Most of these sites are lower to intermediate altitude sites in the dataset (below 2700 m a.s.l) because elevation is correlated with temperature. Sodium ions (Na^+) largely follow the same axis as MJT as evaporation is related in part to temperature. In summary, MJT and Cl^- are both independent variables that drive the second CCA axis and Cl^-, and Na^+

partially reflect evaporation effects because, on average, lakes in warmer climates evaporate more than those in colder ones. In addition, Cl^- concentration may also relate to the characteristics of the bedrock geology of the region. We highlight that there are very few lakes on the Cl^- gradient and these lakes are from the border of Sichuan and Yunnan Provinces, where geothermal springs are widespread. We argue that developing a MJT transfer function is appropriate for this large~~he 100~~ lake training set because MJT is independent of other variables (e.g. Rees et al., 2008; Chang et al., 2015a). Although Cl^- is also independent and co-dominates CCA axis 2, the overall explanatory power is lower (Table 2~~b~~) and also the lambda ratio (λ1/λ2) is smaller~~less~~ than MJT (Table 3~~b~~). We retained all 100 lakes from the region without removing sites to artificially enhance the MJT gradient in the ordination analyses and model development because this large ~~100 lake~~ dataset is an ~~a more~~ accurate reflection of the natural environment of south-western~~SW~~ China.

~~We re-highlight that some chironomid taxa appeared as stenotherms in the 47 lake dataset only because the dataset does not cover the full environmental range. For example, the CCA bi-plot for the 47 lake training set indicating that *Tanytarsus gracilentus*-type, *Tvetenia tamafalva*-type and *Micropsectra* follow the MJT gradient closely (Fig 3a). In the 100 lake training set, we observed that *Tanytarsus gracilentus*-type is more closely related to lake depth, while both *Tvetenia tamafalva*-type and *Micropsectra* show closer correlation with LOI and Cl^- instead of MJT. The latter observations match with the ecological recognition and interpretation of these taxa in literature where *Tanytarsus gracilentus*-type was identified as a benthic species in the arctic (Einarsson et al., 2004; Ives et al., 2008); *Tvetenia tamafalva*-type was often found in streams and this is likely related to the organic content (LOI) of the substrates as they are detritus feeders (Brennan and McLachlan, 1979); while *Micropsectra* was found in thermal springs and pools (Hayford et al., 1995; Batzer and Boix, 2016) and this is reflected in this dataset with having a close relationship with Cl^-. It presents in lakes such as Lake Tengchongqinghai, Qicai Lake and Lake Haizibian that have high levels of Cl^- ions. These sites are located in geothermal spring region of Sichuan and Yunnan Provinces.~~

~~Well-known warm stenotherms that are distributed along the MJT gradient of the CCA species bi-plot (Fig. 3c) for the 100 dataset include *Dicrotendipes*, *Microchironomus*, *Polypedilum* and *Microtendipes*. Many studies (e.g. Walker et al. 1991; Larocque et al. 2001; Rosenberg et al., 2004; Brodersen and Quinlan, 2006; Woodward and Shulmeister, 2006) show that these taxa are warm temperature indicators worldwide. We therefore further argue that while MJT explained a higher total variance in the chironomid data in the 47 Yunnan lake training set, the 100 lake training set has a clear advantage in that it contains a more complete range of temperatures and environments expected to have been experienced by lakes and their chironomid fauna in the past (Brooks and Birks, 2001). This will be particularly useful when applying the models to reconstruct changes in the late Pleistocene and Holocene when climates were different (Heiri et al., 2011).~~

~~5.3 Comparisons of the transfer function statistics~~

~~We compared the statistical results of the transfer functions generated from the 47 and 100 lakes training sets.~~ We selected the WA-PLS based transfer function models over the WAinv based approach for both training sets because the addition of PLS components can reduce the prediction error in datasets with moderate to large noise (ter Braak and Juggins, 1993). ~~The 47 lake dataset WA-PLS model yields a strong r^2_{jack} (0.83) and a comparably lower $RMSEP_{jack}$ (1.7 °C, represents 12.8% of scalar length of the MJT gradient). The performance of the model is highly comparable to models of a similar kind worldwide such as from eastern North America with 136 lakes (r^2 = 0.82, Barley et al., 2006) and Finland with 77 lakes (r^2 = 0.78, Luoto, 2009) where the RMSEPs represent 11.7% and 12.5% of their respective temperature gradient length. However, there are apparent caveats in the distribution of the model predicted MJTs and error residuals along the temperature gradient (Fig.4a-d). These include: (1) there is a gap in sites between the MJTs of 12 and 15 °C; (2) there is a wide scatter of error residuals for sites located in an intermediate temperature range (between 10 and 12 °C) and at the warmer end (> 18 °C). These indicate there are limitations for the model to accurately reconstruct temperatures in warmer conditions (e.g. the Holocene) and during relatively minor cooling events (e.g. the Little Ice Age). The 47 lakes training set covers a MJT gradient of 13.2 °C and this should be capable of detecting glacial to interglacial changes. The problem in the smaller data set is that some taxa are likely to have their climate tolerances and optima significantly underestimated (Heiri et al., 2011). For example, *Diamesa*, is present up to a MJT of 10 °C in the 47 lake dataset, whereas in the 100 lake dataset, it is present in samples with a MJT of 17 °C. The consequence of this is that *Diamesa* appears as a cold stenotherm in the 47 lakes dataset but it is actually cosmopolitan. This finding is in line with Heiri et al. (2011) and Brooks and Birks (2001), who demonstrated from Europe that broader datasets give a more accurate view of the chironomid distribution data.~~

The ~~100 lakes~~ training set ~~extends the~~has a MJT gradient ~~by 3.4 °C to~~of 16.6 °C and the RMSEP represents 13.8% of the scalar length of the MJT gradient. This is ~~still~~ comparable with most chironomid-based transfer function models including ~~transfer function models~~those developed from Northern Sweden with 100 lakes (r^2 = 0.65, Larocque et al., 2001), ~~and~~ western Ireland with 50 lakes (r^2 = 0.60, Potito et al., 2014) and Finland with 77 lakes (r^2 = 0.78, Luoto, 2009)~~,~~ representing 14.7%, ~~and~~ 15% and 12.5% of the scala~~e~~r length of the temperature gradient respectively but less robust than the combined 274-lakes transfer function developed from Europe (r^2 = 0.84, RMSEP representing 10.4% of the scalar length of the MJT gradient) (Heiri et al., 2011). Despite of the relatively lower model coefficient (r_{boot} = 0.63), we observe that by ~~increasing the~~having a large number of lakes in the calibration set, the distribution of the sites along the MJT gradient is relatively even~~ed out~~ (Fig. 4d). The distribution of the error residuals generates a smooth~~smoother~~ curve (Fig. 4d)~~ than the 47 lakes training set~~. The model leads to overestimation of low and underestimation of high temperature values which is typical of the WA models (ter Braak and Juggins, 1993). We acknowledge that the lower model coefficient (r_{boot}) may also relate to the low~~ered~~ explanatory power of MJT in the chironomid species data and ~~increased~~ large number of independent and significant variables in the ~~100 lake~~ training set when a wide~~r~~ range of lakes were included. However, ~~increasing the length of the~~the extensive temperature gradient length allowed the incorporation of full potential abundance and distributional ranges for each of the chironomid taxa.

5.2~~4~~ Tiancai Lake reconstructions

~~The 47 lakes training set displays an apparently stronger statistical correlation to the temperature record. We argue that the increased robustness of applying the transfer function model based on the larger dataset outweigh the modest reduction in statistical performance.~~ All three types of diagnostic techniques applied (Fig 6 b-d) suggest that a reliable MJT reconstruction was provided by the two-component WA-PLS model based on this~~e~~ 100-~~-~~lake dataset overall. We highlight that the eight samples from the years between 2000 and 2007 AD have 'poor' and 'very poor' fit to MJT may suggest that it is possible a second gradient other than MJT influencing the chironomid species distribution and abundance in the most recent fossil samples of Tiancai Lake. ~~We also predict that the model based on the larger dataset may amplify both cool and warm events because it covers a more complete environmental range, allowing taxon responses to be fully observed. In order to test this and also to test whether either reconstruction matches reality, we applied both of the WAPLS models to the Tiancai Lake chironomid data, for the period between 1860 AD and the present.~~

~~We plot the trends of MJT reconstruction results from both the WAPLS models against the ~50-year long instrumental record from Lijiang station (Fig. 6e).~~ In the comparison for the MJT reconstruction results with the instrumental record from Lijiang weather station (Fig. 6a), w~~W~~e do not expect the absolute MJT values to be identical because Lijiang is located ~55 km east-northeast (ENE) and ~1600 m lower in altitude than Tiancai Lake. We applied a typical environmental lapse rate of temperature (change with altitude) for Alpine regions, which is 0.58 °C per 100 metres (Rolland, 2003) to estimate the equivalent MJT values from Lijiang station. If the chironomid-~~-~~based transfer functions are able to provide reliable estimates for MJT~~s~~, we expect the records demonstrate a similar trend with the instrumental data (Fig. 6e).

The reconstruction results are well matched with the expected outcomes~~: (1) It is reassuring that~~ as the transfer function models based on 100 lakes ~~dataset~~ for ~~a broader~~the broad area of south-western~~SW~~ China reconstructs ~~mean July temperatures (~~MJT~~s) with a similar pattern to the 47 Yunnan lakes dataset in terms of the trend; (2) as expected, the WAPLS model based on the 100 dataset amplifies both cool and warm periods; (3) both chironomid based reconstructions~~ broadly match the trend recorded by the instrument. By applying the environmental lapse rate, we observe a temperature depression from Lijiang to Tiancai Lake of about 9.3 °C (giving an inferred MJT at Tiancai Lake of 8.1 ~~8.4~~°C in the year of 2004). This magnitude of change is consistent with the chironomid-based reconstructions from Tiancai Lake (at an average of 7.8 °C for the samples representing the years of 2004-2005), where the difference in mean is 0.3~~0.67~~ °C ~~(equivalent to a MJT of 7.7 °C)~~ when compared ~~to the results derived from the 100 lake based WAPLS model and 0.86 °C (equivalent MJT of 7.5 °C) for the 47 lake model~~. The implication is that the ~~100 lake based model~~transfer function model is~~may be~~ able to reconstruct the MJT~~s~~ that closely ~~better~~ reflects the actual climate record~~, though the difference between the models is small~~. We observe there are minor out of phase patterns (Fig. 6e) and this may reflect the uncertainties of applying the ^{210}Pb chronology to very recent lake sediments (Binford, 1990). Furthermore, we note that sediment samples reflect more than one season and consequently the total range of the temperature reconstructions from the chironomid samples is likely to be slightly less than the meteorological data because of the smearing out of extreme years. While we expect overall trends between Lijiang and Tiancai Lake to be similar, the sites are not closely co-located and some natural variability between the sites is expected. Nevertheless, a~~A~~ significant correlation ($p <$ 0.05~~, r = 0.45, n = 31~~) was ~~still~~ obtained between the instrumental data and the ~~100 lake~~ WA-PLS model inferred MJT data for the last ~ 50 years. We highlight that in addition to the record validation produced by the reconstruction diagnostic techniques, the well-compared trend with the instrumental record is reassuring that the model is capable to provide realistic pattern of the long-term mean July temperature changes. In summary, the chironomid~~e WAPLS model-~~-based transfer function developed using~~on~~ the 100 ~~-~~lakes calibration~~chironomid~~ training set has ~~produced~~ generated reliable ~~summer~~ quantitative temperature records and can ~~realistically also~~ be applied to reconstructing past climate in south-western ~~SW~~ China.

6 Conclusions

~~Two c~~Chironomid-~~-~~based summer temperature transfer functions using 100 lakes from south-western China have been constructed and applied to Yunnan region in the south-eastern margin of the Tibetan Plateau~~SW China~~. ~~These include transfer functions based on a 47 lakes training set confined to Yunnan and a 100 lakes training set from a broader region of south-western China. The first component of WA-PLS model based on the 47 lakes training set produced an~~ ~~r^2_{jack} of 0.83, AveBiasjack of 0.11, a MaxBiasjack of 3.15 and RMSEP of 1.72 °C. The second component of WA-PLS bootstrap model for the 100 lakes training set is the most robust for those data and produced an~~ ~~r^2_{boot} of 0.63, AveBiasboot of 0.10, a MaxBiasboot of 5.16 and RMSEP (s1 + s2) of 2.31 °C (whereas RMSEs1 = 0.88 °C and RMSEs2 = 2.14 °C).~~ Both the ordination and transfer function statistics show that ~~the 47 lakes training set has a stronger correlation with MJT, but in practice, we demonstrated that the reconstruction results based on~~ the chironomid-based ~~100 lakes training set are also~~transfer function is reliable. ~~The larger dataset may potentially provide a better representation of the environmental preferences of the chironomid taxa.~~ This~~e~~ ~~100 lakes~~large regional training set allowed insight into the regional chironomid distribution and species abundance despite having many more independent environmental gradients. The test of the ~~two~~ transfer function models against the modern data suggest that the two-component WA-PLS model~~s~~ provided ~~near identical~~ reconstructions that match the trend of the local instrumental record for the last 50 years. As also demonstrated from pan-European chironomid based transfer functions (e.g. Brooks and Birks, 2001; Heiri et al., 2011), this~~e~~ broadly based 100 ~~SW~~ Chinese lakes is likely ~~more~~ robust and is ~~equally~~ appropriate for use reconstructing long-term summer temperature changes of south-western~~SW~~ China**.**

Acknowledgement: We thank X Chen, E.F. Liu, M. Ji, R. Chen, Y.L. Li, J.J. X.Y. Xiao, Wang, Q. Lin and B.Y. Zheng (Nanjing Institute of Geography and Limnology, Chinese Academy of Sciences) for field assistance, Jürgen Böhner (Georg-August-University Göttingen, Germany) for help with climate data.~~,~~ This research was supported by the Program of Global Change and Mitigation (2016YFA0600502), the National Natural Science Foundation of China (No. 41272380, 41572337).

References

Appleby, P.G., 2001.Chronostratigraphic techniques in recent sediment, In: Last WM, Smol J P. Tracking environmental change using lake sediments, Volume 1: basin analysis, coring, and chronological techniques. Klauwer Academic Publishers, pp. 171-196.

Appleby, P.G., Oldfield, F., 1992. Application of 210Pb to sedimentation studies. In: Ivanovich M, Harmon RS (Eds.), Uranium series disequilibrium. OUP, pp. 731-778.

Batzer, D., Boix, D., 2016. Invertebrates in Freshwater Wetlands: An International Perspective on their Ecology. Springer. pp. 361 – 370.

Barley, E.M., Walker, I.R., Kurek, J., Cwynar, L.C., Mathewes, R.W., Gajewski, K., Finney, B.P., 2006. A northwest North American training set: Distribution of freshwater midges in relation to air temperature and lake depth. Journal of Paleolimnology 36, 295-314

Binford, M.W., 1990. Calculation and uncertainty analysis of 210Pb dates for PIRLA project lake sediment cores. Journal of Paleolimnology 3, 253-267.

Birks, H.J.B., 1998. Numerical tools in paleolimnology progress, potentialities, and problems. Journal of Paleolimnology 20, 307–332.

Birks, H.J.B., 1995. Quantitative palaeoenvironmental reconstructions. In: Maddy, D., Brew, J.S. (Eds.), Statistical Modelling of Quaternary Science Data. Technical Guide 5. Quaternary Research Association, Cambridge, pp. 116–254

Böhner J., 1994. Circulation and representativeness of precipitation and air temperature in the southeast of the Qinghai-Xizang Plateau. GeoJournal 34, 55-66.

Böhner, J., 2006. General climatic controls and topoclimatic variations in Central and High Asia. Boreas 35, 279-295.

Böhner, J., Lehmkuhl, F., 2005. Environmental change modelling for Central and High Asia: Pleistocene, present and future scenarios. Boreas 34, 220-231.

Brennan, A., McLachlan, A.J., 1979. Tubes and tube-building in a lotic Chironomid (Diptera) community. Hydrobiologia 67, 173-178.

Brodersen, K.P., Quinlan, R., 2006. Midges as palaeoindicators of lake productivity, eutrophication and hypolimnetic oxygen. Quaternary Science Reviews 25, 1995-2012.

Brooks, S.J., Birks, H.J.B., 2001. Chironomid-inferred air temperatures from Lateglacial and Holocene sites in north-west Europe: progress and problems. Quaternary Science Reviews 20, 1723-1741.

Brooks, S.J., Davies, K.L., Mather, K.A., Matthews, I.P., Lowe, J.J., 2016. Chironomid-inferred summer temperatures for the Last Glacial–Interglacial Transition from a lake sediment sequence in Muir Park Reservoir, west-central Scotland. Journal of Quaternary Science 31, 214-224.

Brooks, S.J., Langdon, P.G., Heiri, O., 2007. The Identification and Use of Palaearctic Chironomidae Larvae in Palaeoecology. Quaternary Research Association.

Chang, J.C., Shulmeister, J., Woodward, C., 2015. A chironomid based transfer function for reconstructing summer temperatures in southeastern Australia. Palaeogeography, Palaeoclimatology, Palaeoecology 423, 109-121.

Chang, J.C., Shulmeister, J., Woodward, C., Steinberger, L., Tibby, J., Barr, C., 2015. A chironomid-inferred summer temperature reconstruction from subtropical Australia during the last glacial maximum (LGM) and the last deglaciation. Quaternary Science Reviews 122, 282-292.

Cranston. P.S., 1995. Chironomids: from Genes to Ecosystems, CSIRO, Melbourne, pp. 482.

Cranston, P.S., 2000. Electronic guide to the chironomidae of Australia. http://www.science.uts.edu.au/sasb/chiropage/

Dean Jr, W.E., 1974. Determination of carbonate and organic matter in calcareous sediments and sedimentary rocks by loss on ignition: comparison with other methods. Journal of Sedimentary Research, 44, 242-248.

Dykoski, C.A., Edwards, R.L., Cheng, H., Yuan, D., Cai, Y., Zhang, M., Lin, Y., Qing, J., An, Z., Revenaugh, J., 2005. A high-resolution, absolute-dated Holocene and deglacial Asian monsoon record from Dongge Cave, China. Earth and Planetary Science Letters 233, 71-86.

Eggermont, H., Heiri, O., Russell, J., Vuille, M., Audenaert, L., Verschuren, D., 2010. Paleotemperature reconstruction in tropical Africa using fossil Chironomidae (Insecta: Diptera). Journal of Paleolimnology 43, 413-435.

Einarsson, Á., Stefánsdóttir, G., Jóhannesson, H., Ólafsson, J.S., Már Gíslason, G., Wakana, I., Gudbergsson, G., Gardarsson, A., 2004. The ecology of Lake Myvatn and the River Laxá: Variation in space and time. Aquatic Ecology 38, 317-348.

Fortin, M.C., Medeiros, A.S., Gajewski, K., Barley, E.M., Larocque-Tobler, I., Porinchu, D.F., Wilson, S.E., 2015. Chironomid-environment relations in northern North America. Journal of Paleolimnology 54, 223-237.

Gajewski, K., Bouchard, G., Wilson, S.E., Kurek, J., Cwynar, L.C., 2005. Distribution of Chironomidae (Insecta: Diptera) Head Capsulesin Recent Sediments of Canadian Arctic Lakes. Hydrobiologia 549, 131-143.

Hall, R.I., Smol, J.P., 1992. A weighted—averaging regression and calibration model for inferring total phosphorus concentration from diatoms in British Columbia (Canada) lakes. Freshwater Biology 27, 417-434.

Hayford, B.L., Sublette, J.E., Herrmann, S.J., 1995. Distribution of Chironomids (Diptera: Chironomidae) and Ceratopogonids (Diptera: Ceratopogonidae) along a Colorado Thermal Spring Effluent. Journal of the Kansas Entomological Society 68, 77-92.

Heiri, O., Brooks, S.J., Birks, H.J.B., Lotter, A.F., 2011. A 274-lake calibration data-set and inference model for chironomid-based summer air temperature reconstruction in Europe. Quaternary Science Reviews 30, 3445-3456.

Heiri, O., Lotter, A.F., Hausmann, S., Kienast, F., 2003. A chironomid-based Holocene summer air temperature reconstruction from the Swiss Alps. The Holocene 13, 477-484.

Hill, M.O., Gauch, H.G., 1980. Detrended Correspondence Analysis: An Improved Ordination Technique. Vegetatio 42, 47–58.

Hinkley, T.K., 1996. Preferential Weathering of Potassium Feldspar in Mature Soils, Earth Processes: Reading the Isotopic Code. American Geophysical Union, pp. 377-389.

Holmes, N., Langdon, P.G., Caseldine, C., Brooks, S.J., Birks, H.J.B., 2011. Merging chironomid training sets: implications for palaeoclimate reconstructions. Quaternary Science Reviews 30, 2793-2804.

Ives, A.R., Einarsson, A., Jansen, V.A.A., Gardarsson, A., 2008. High-amplitude fluctuations and alternative dynamical states of midges in Lake Myvatn. Nature 452, 84-87.

Kim, N., Han, J.K., 1997. Assessing the integrity of cross-validation: a case for small sample-based research. Hong Kong University of Science and Technology, Department of Marketing, Working Paper Series no. MKTG 97.096

Langdon, P.G., Holmes, N., Caseldine, C.J., 2008. Environmental controls on modern chironomid faunas from NW Iceland and implications for reconstructing climate change. Journal of Paleolimnology 40, 273-293.

Larocque, I., Hall, R.I., Grahn, E., 2001. Chironomids as indicators of climate change: a 100 ‐ lake training set from a subarctic region of northern Sweden (Lapland). Journal of Paleolimnology 26, 307-322.

Lotter, A.F., Walker, I.R., Brooks, S.J., Hofmann, W., 1999. An intercontinental comparison of chironomid palaeotemperature inference models: Europe vs North America. Quaternary Science Reviews 18, 717-735.

Luoto, T.P., 2009. A Finnish chironomid- and chaoborid-based inference model for

reconstructing past lake levels. Quaternary Science Reviews 28, 1481-1489.
Luoto, T.P., Kaukolehto, M., Weckström, J., Korhola, A., Väliranta, M., 2014. New evidence of warm early-Holocene summers in subarctic Finland based on an enhanced regional chironomid-based temperature calibration model. Quaternary Research 81, 50-62.
Institute of Geography, Chinese Academy of Sciences, 1990. Atlas of Tibet Plateau. Science Press. (in Chinese).
Juggins, S., 2005. C2 Version 1.5: software for ecological and palaeoecological data analysis and visualisation. University of Newcastle, Newcastle-upon-Tyne.
Juggins, S., 2013. Quantitative reconstructions in palaeolimnology: new paradigm or sick science? Quaternary Science Reviews 64, 20-32.
Meunier, A. and Velde, B.D., 2013. Illite: Origins, evolution and metamorphism. Springer Science & Business Media, pp. 65 – 76.
Muschitiello, F., Pausata, F.S.R., Watson, J.E., Smittenberg, R.H., Salih, A.A.M., Brooks, S.J., Whitehouse, N.J., Karlatou-Charalampopoulou, A., Wohlfarth, B., 2015. Fennoscandian freshwater control on Greenland hydroclimate shifts at the onset of the Younger Dryas. Nature Communications 6.
Oliver, D.R., Roussel, M.E. 1982. The larvae of Pagastia Oliver (Diptera: Chironomidae) with descriptions of three new species. The Canadian Entomologist, 114: 849–854.
Potito, A.P., Woodward, C.A., McKeown, M., Beilman, D.W., 2014. Modern influences on chironomid distribution in western Ireland: potential for palaeoenvironmental reconstruction. Journal of Paleolimnology 52, 385-404.
Quinlan, R., Smol, J.P., 2001. Setting minimum head capsule abundance and taxa deletion criteria in chironomid-based inference models. Journal of Paleolimnology 26, 327-342.
Rees, A.B.H., Cwynar, L.C., 2010. Evidence for early postglacial warming in Mount Field National Park, Tasmania. Quaternary Science Reviews 29, 443-454.
Rees, A.B.H., Cwynar, L.C., Cranston, P.S., 2008. Midges (Chironomidae, Ceratopogonidae, Chaoboridae) as a temperature proxy: a training set from Tasmania, Australia. Journal of Paleolimnology 40, 1159-1178.
Renberg, I., 1991. The HON-Kajak sediment corer. Journal of Paleolimnology 6, 167-170.
Rieradevall, M., Brooks, S.J., 2001. An identification guide to subfossil Tanypodinae larvae (Insecta: Diptera: Chrironomidae) based on cephalic setation. Journal of Paleolimnology 25, 81-99.
Rolland, C., 2003. Spatial and Seasonal Variations of Air Temperature Lapse Rates in Alpine Regions. Journal of Climate 16, 1032-1046.
Rosenberg, S.M., Walker, I.R., Mathewes, R.W., Hallett, D.J., 2004. Midge-inferred Holocene climate history of two subalpine lakes in southern British Columbia, Canada. The Holocene 14, 258-271.
Samartin, S., Heiri, O., Vescovi, E., Brooks, S.J., Tinner, W., 2012. Lateglacial and early Holocene summer temperatures in the southern Swiss Alps reconstructed using fossil chironomids. Journal of Quaternary Science 27, 279-289.
Tang, H. Q. 2006. Biosystematic study on the chironomid larvae in China (Diptera:

Chironomidae). Nankai University, Tianjin, China, 945pp.

ter Braak, C. J. F., 1987. Unimodal models to relate species to environment. Agricultural Mathematics Group, Wageningen, The Netherlands. pp. 152

ter Braak, C.J.F., Juggins, S., 1993. Weighted averaging partial least squares regression (WA-PLS): an improved method for reconstructing environmental variables from species assemblages. Hydrobiologia 269, 485-502.

ter Braak, C.J.F., Šmilauer, P., 2002. CANOCO reference manual and CanoDraw for Windows user's guide: software for canonical community ordination (version 4.5), Microcomputer power, Itaca, www.canoco.com.

Walker, I. R., 2001. Midges: Chironomidae and related Diptera. In: J. P. Smol, H. J. B. Birks, and W. M. Last (Eds), Tracking Environmental Change Using Lake Sediments. Volume 4. Zoological Indicators. Kluwer Academic Publishers, Dordrecht. pp. 43-66.

Walker, I.R., Smol, J.P., Engstrom, D.R., Birks, H.J.B., 1991. An Assessment of Chironomidae as Quantitative Indicators of Past Climatic Change. Canadian Journal of Fisheries and Aquatic Sciences 48, 975-987.

Wang, Y.J., Cheng, H., Edwards, R.L., An, Z.S., Wu, J.Y., Shen, C.C., Dorale, J.A., 2001. A High-Resolution Absolute-Dated Late Pleistocene Monsoon Record from Hulu Cave, China. Science 294, 2345-2348.

Wang, Y., Cheng, H., Edwards, R.L., Kong, X., Shao, X., Chen, S., Wu, J., Jiang, X., Wang, X., An, Z., 2008. Millennial- and orbital-scale changes in the East Asian monsoon over the past 224,000 years. Nature 451, 1090-1093.

Wiederholm T., 1983. Chironomidae of the Holarctic region. Keys and diagnoses. Part 1 Larvae. In: Wiederholm T (ed). Scandinavian Entomology Ltd, 1-482.~~Wiederholm, T., 1984. Incidence of deformed chironomid larvae (Diptera: Chironomidae) in Swedish lakes. Hydrobiologia 109, 243-249.~~

Woodward, C.A., Shulmeister, J., 2006. New Zealand chironomids as proxies for human-induced and natural environmental change: Transfer functions for temperature and lake production (chlorophyll a). Journal of Paleolimnology 36, 407-429.

Woodward, C.A., Shulmeister, J., 2007. Chironomid-based reconstructions of summer air temperature from lake deposits in Lyndon Stream, New Zealand spanning the MIS 3/2 transition. Quaternary Science Reviews 26, 142-154.

Xiao, X., Haberle, S.G., Shen, J., Yang, X., Han, Y., Zhang, E., Wang, S., 2014. Latest Pleistocene and Holocene vegetation and climate history inferred from an alpine lacustrine record, northwestern Yunnan Province, southwestern China. Quaternary Science Reviews 86, 35-48.

Zhang, E., Bedford, A. Jones,R., Shen, J., Wang, S., Tang, H., 2006. A subfossil chironomid-total phosphorus inference model from the middle and lower reaches of Yangtze River lakes. Chinese Science Bulletin. 51: 2125-2132

Zhang, E., Cao, Y., Langdon, P., Jones, R., Yang, X., Shen, J., 2012. Alternate trajectories in historic trophic change from two lakes in the same catchment, Huayang Basin, middle reach of Yangtze River, China. Journal of Paleolimnology 48, 367-381.

Zhang, E., Jones, R., Bedford, A., Langdon, P., Tang, H., 2007. A chironomid-based salinity inference model from lakes on the Tibetan Plateau. Journal of Paleolimnology 38, 477-491.

Zhang, E., Langdon, P., Tang, H., Jones, R., Yang, X., Shen, J., 2011. Ecological influences affecting the distribution of larval chironomid communities in the lakes on Yunnan Plateau, SW China. Fundamental and Applied Limnology 179, 103-113.
Zhang, E., Liu, E., Jones, R., Langdon, P., Yang, X., Shen, J., 2010. A 150-year record of recent changes in human activity and eutrophication of Lake Wushan from the middle reach of the Yangze River, China. Journal of Limnology 69, 235-241.

FIGURE LEGENDS

Fig. 1 Map of south-west China (a) showing the location of 100 lakes included in ~~full~~ the calibration training set (square box). (b) Lakes from Yunnan Province are shown in the square box and (c) the location of Tiancai Lake is marked with yellow triangle. ~~The subset of 47 lakes from Yunnan province is shown in the square box (b). The triangle ( ) indicates the location of Tiancai Lake in (c).~~

Fig 2a. Chironomid species stratigraphy~~percent~~ diagram of the ~~9~~85 non-rare taxa with ~~N and~~ N_2 > 2. Mean July temperature is on the y-axis and taxon abundance is in percentage~~Lake number from 1 to 100 is on the y-axis~~. The taxon code is correspondent to the code used in Figure 3a. Warm and cold stenotherms were identified and grouped based on optical observation and the ~~canonical correspondence analysis (CCA) species scores~~Beta coefficient (from low to high) calculated based on the bootstrap weighted average partial least square (WA-PLS) model for each species in C2 software (Juggins, 2005).

Fig 2b. Forty-one (41) non-rare chironomid species present in the short core (28 cm) from Tiancai Lake where the calibrated ^{210}Pb based age is on the y-axis and taxon abundance is in percentage.

Fig 3 CCA bip-lots of sample and species scores constrained to environmental variables that individually explain a significant ($p < 0.05$) proportion of the chironomid species data. (a) species and (b) sample scores constrained to ~~eight~~ seven significant environmental variables in ~~the 47 Yunnan lakes training set. (c) species and (d) sample scores constrained to seven significant variables in~~ the 100 lakes of southwestern China. The species codes are correspondent to the taxa names shown in Fig. 2a.

Fig 4 Performance of the weighted average models with inverse deshrinking (WAinv) and partial least square (WA-PLS) models using the ~~47 lakes and~~ 100 lakes calibration data sets: (a) WAinv ~~jackknifed~~ bootstrap model ~~with 47 lakes~~ (b) the second component of the WA-PLS bootstrap~~jackknifed~~ model ~~with 47 lakes (c) WAinv bootstrapped model with 100 lakes and (d) WA-PLS bootstrapped model with 100 lakes~~. Diagrams on the left show the predicted versus observed mean July temperature (MJT) and diagrams on the right display residuals of the predicted versus observed mean July temperature. Note that both ~~all the~~ models have a tendency to over-predict temperatures from the cold end of the gradient and underestimate temperatures at the warm end. This is typical for the WA based models.

Fig 5 The age and depth model for ^{210}Pb dating results of the short core (28~~30~~ cm) from Tiancai Lake. The concentration of ^{137}Cs (circle), excess ^{210}Pb (triangle) and the calibrated age (AD years) (square) were plotted against core sample depth, respectively.

Fig 6 (a) Chironomid-based mean July temperature (MJT) reconstruction results from Tiancai Lake based on two~~4~~ transfer function models: solid black~~red~~ line is the reconstruction based on the weighted average partial least square (WA-PLS) bootstrap~~ped~~ model with two~~2~~ components ~~using 100 lakes calibration set~~, dashed~~solid~~ black line is the reconstruction based on the ~~WAPLS jackknifed model with 1 component using 47 lakes in Yunnan, dashed black line is based on the~~ weighted average with inverse deshrinking (WAinv) ~~jackknifed~~ bootstrap model ~~using 47 lakes in Yunnan and dashed red line is based on WAinv jackknifed model using 100 lakes in southwestern China~~. Red solid line is the instrumental data from Lijiang weather station, corrected applying the lapse rate and solid grey line is the three-sample moving average of the dataset. Reconstruction of diagnostic statistics for the 100 lake dataset where (b) displays the goodness-of-fit statistics of the fossil samples with ~~mean July temperature (~~MJT~~)~~. Dashed lines are used to identify samples with 'poor fit' (> 95th percentile) and 'very poor fit' (> 90th percentile) with temperature (c) Nearest modern analogues for the fossil samples in the calibration data set, where dashed line is used to show fossil samples with 'no good' (5%) modern analogues. (d) Percentage of chironomid taxa in fossil samples that are rare in the modern calibration data set (Hill's

~~N < 2 and~~ $N_2 < 2$). (e) Comparison between the chironomid-based transfer function reconstructed trends (represented by MJT anomalies) with the instrumental data from Lijiang weather station (in red solid line, with three-sample moving average). Black solid line represents the reconstruction based on the WA-PLS bootstrapped model with two~~2~~ components using 100 lakes calibration set ~~and grey dashed line represents the reconstruction based on the WAPLS bootstrapped model with 1 component using 47 lakes calibration set from Yunnan in this diagram~~.

TABLE LEGENDS

Table 1. List of all the 18 environmental and climate variables measured from 100 south-western Chinese lakes, with mean, minimum and maximum values ~~cited for the 47 lakes calibration set from Yunnan and the full 100 lakes, respectively~~.

Table 2. CCA summary of the seven ~~eight~~ significant variables ($p < 0.05$) including canonical co-efficients and t-values of the environmental variables with the ordination axes including ~~(a) 47 lakes and 53 non-rare species and (b)~~ 100 lakes and 8~~9~~5 non-rare species

Table 3. Partial Canonical Correspondence Analysis (pCCA) result with environmental variables that showed a significant correlation ($p < 0.05$) in CCAs with chironomid species data included ~~, where (a) is based on the 47 lakes training set, where mean July temperature (MJT) (bold) is the only variable retained its significance level (p < 0.01) after each pCCAs and (b) is~~ based on the 100 lakes calibration training set. ~~in which d~~Depth, K+, Cl-, LOI and MJT (bold) maintained~~retained~~ their significance ($p < 0.01$) after each step of the pCCAs.

Table 4. (a) Results of the transfer function output ~~development where (a)~~ shows the performance of the weighted average model with inverse and classical deshrinking (WAinv, WAcla), weighted average partial least squares (WA-PLS) models for reconstructing mean July temperature using ~~(a) 47 lakes from Yunnan and 53 non-rare chironomid species and (b) for using~~ 100 lakes from south-western China and 8~~9~~5 non-rare chironomid species. The bold indicates the models that are tested for reconstructing the mean July temperatures from Tiancai Lake. (b) The t-Test (Two-Sample assuming unequal variances) performed on the RMSEP output values of the WA-PLS component 1 and component 2 shows that the result is significant at $p < 0.05$. This suggests there is a difference between the RMSEP of the two models. We therefore selected the second component of the WA-PLS because it produced a lower RMSEP value.

Figure 1

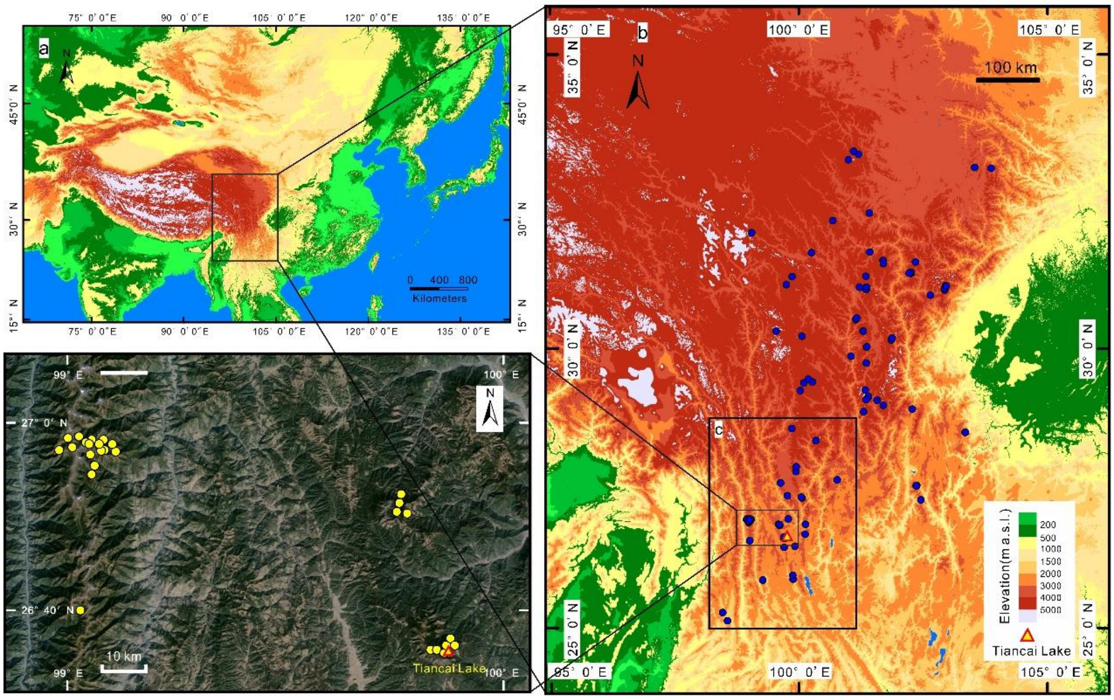

Figure 2a

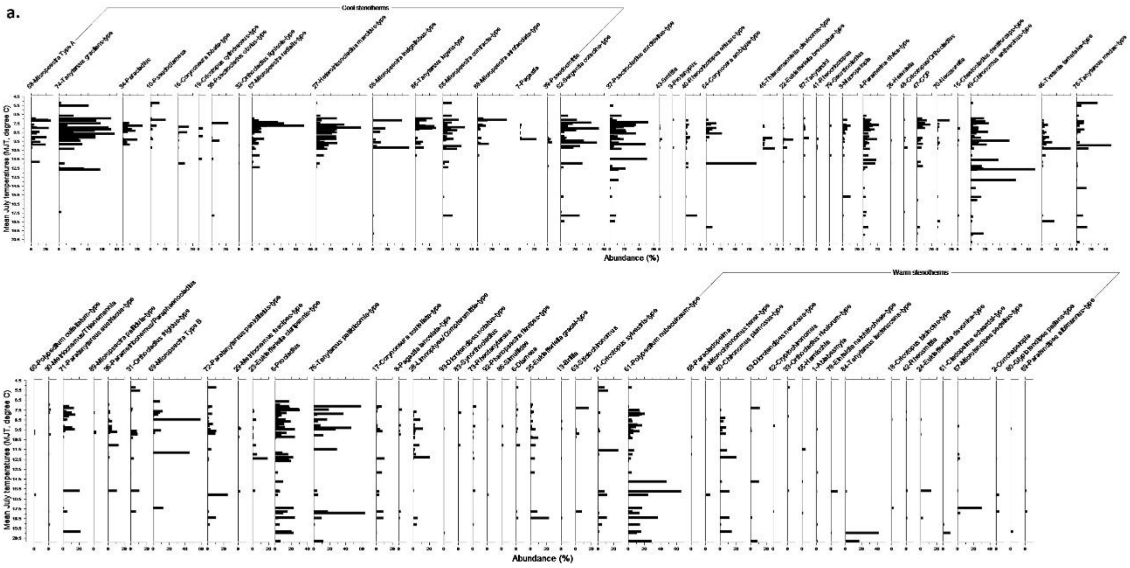

Figure 2b

Figure 3

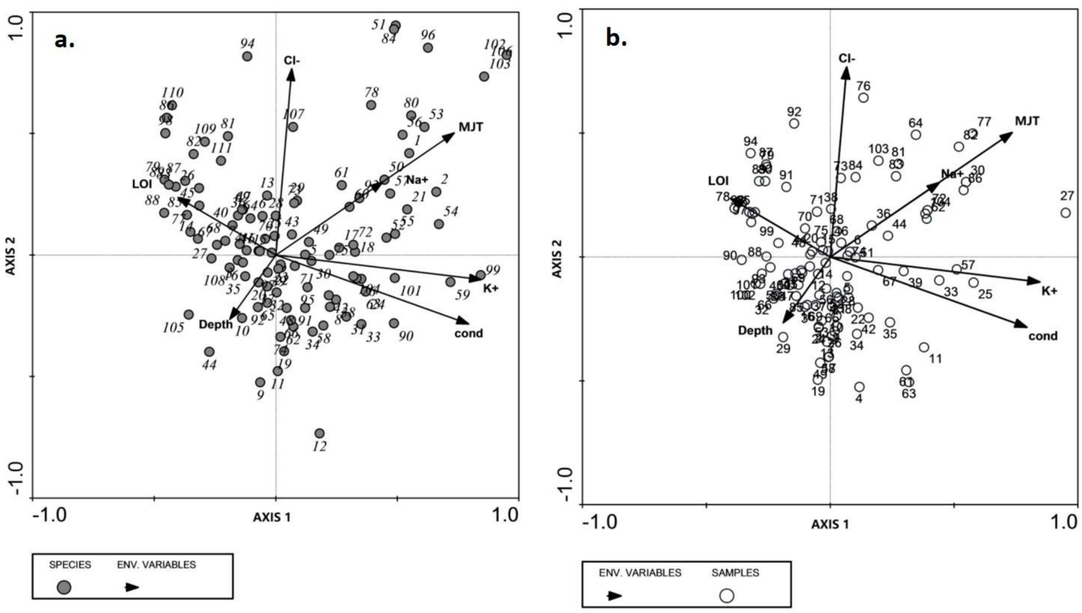

Figure 4

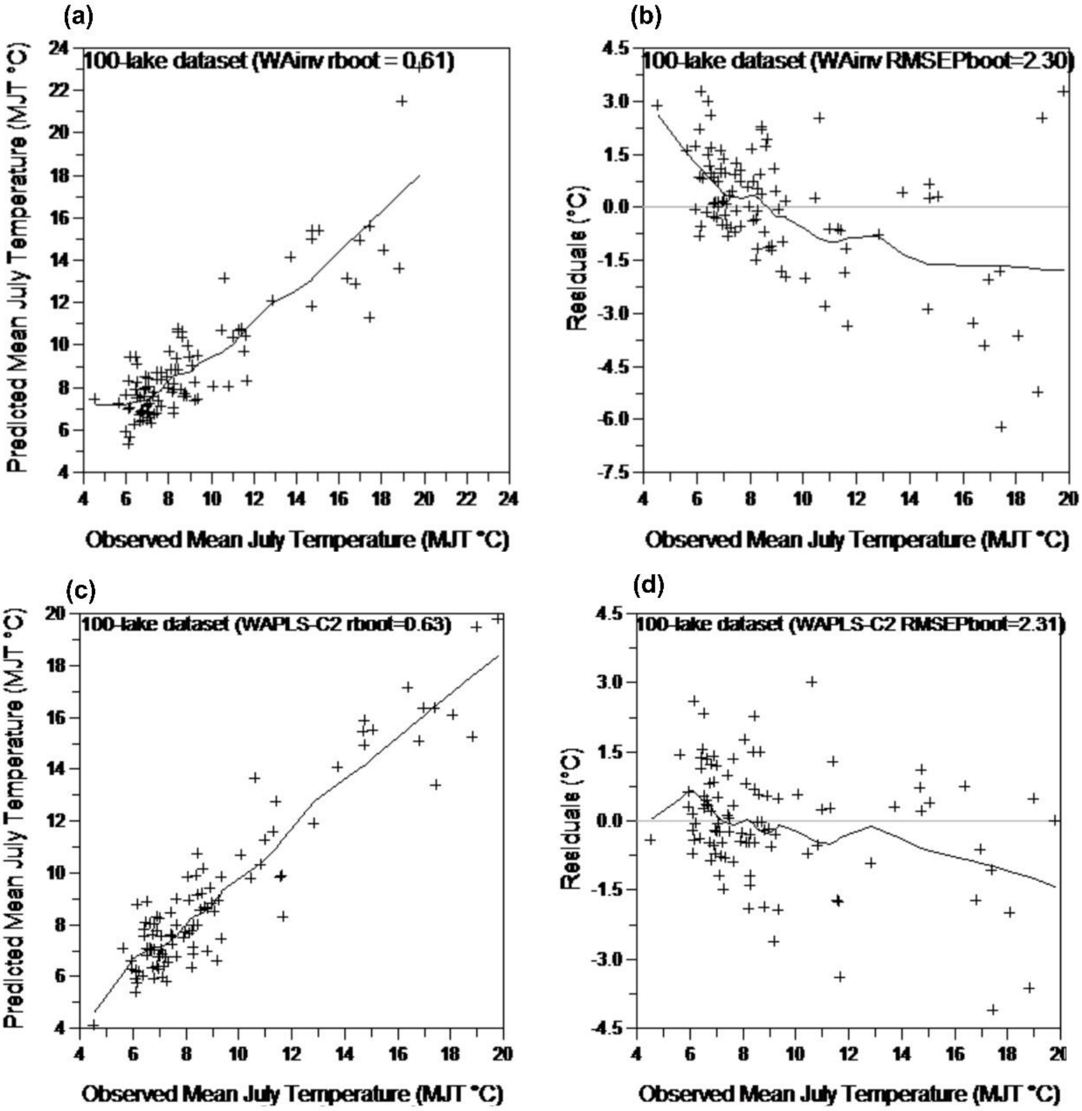
(a)
100-lake dataset (WAinv rboot = 0.61)
Predicted Mean July Temperature (MJT °C)
Observed Mean July Temperature (MJT °C)
(b)
100-lake dataset (WAinv RMSEPboot=2.30)
Residuals (°C)
Observed Mean July Temperature (MJT °C)
(c)
100-lake dataset (WAPLS-C2 rboot=0.63)
Predicted Mean July Temperature (MJT °C)
Observed Mean July Temperature (MJT °C)
(d)
100-lake dataset (WAPLS-C2 RMSEPboot=2.31)
Residuals (°C)
Observed Mean July Temperature (MJT °C)

Figure 5

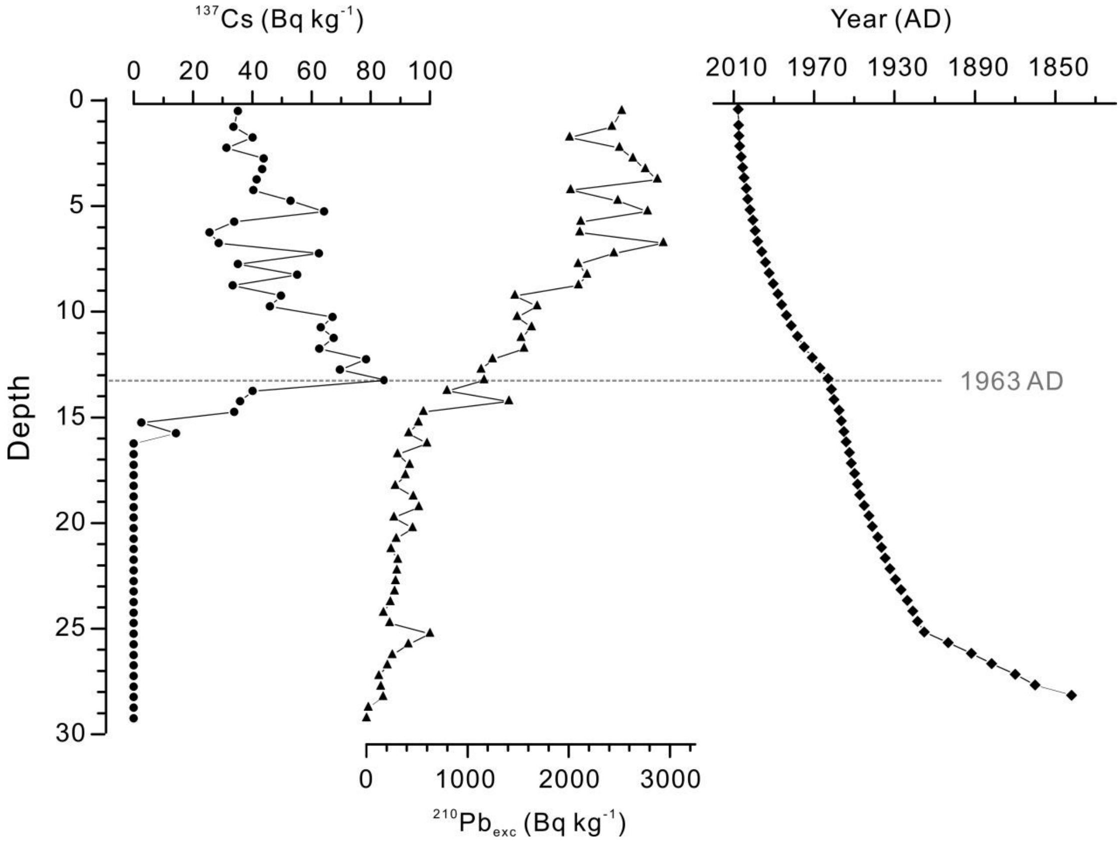

137Cs (Bq kg-1)
0 20 40 60 80 100
Year (AD)
2010 1970 1930 1890 1850
Depth
0
5
10
15
20
25
30
1963 AD
0 1000 2000 3000
210Pbexc (Bq kg-1)

Figure 6

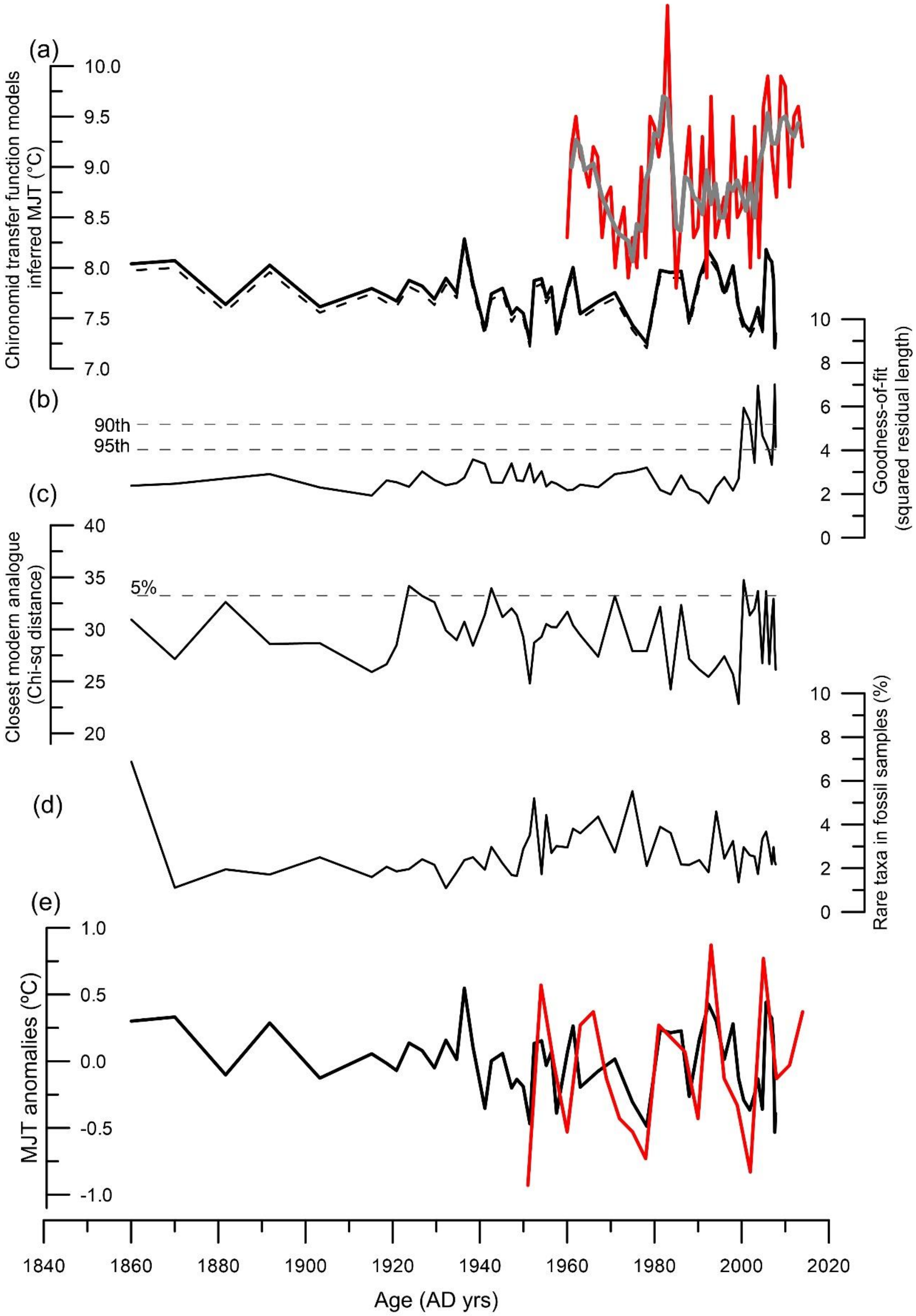
(a)
Chironomid transfer function models inferred MJT (°C)
10.0
9.5
9.0
8.5
8.0
7.5
7.0
(b)
90th
95th
Goodness-of-fit (squared residual length)
10
8
6
4
2
0
(c)
Closest modern analogue (Chi-sq distance)
40
35
30
25
20
5%
(d)
Rare taxa in fossil samples (%)
10
8
6
4
2
0
(e)
MJT anomalies (°C)
1.0
0.5
0.0
-0.5
-1.0
1840
1860
1880
1900
1920
1940
1960
1980
2000
2020
Age (AD yrs)

Table 1

Variable	Unit	Symbol	Mean	Min	Max
Altitude	m	alt	3785	1769	4608
Mean July precipitation	mm	MJP	392	104	1055
Mean annual precipitation	mm	MAP	1820	505	5228
Mean July temperature	°C	MJT	9.1	4.2	19.8
Secchi depth	m	SD	3.5	0.2	12.5
Conductivity	$\mu m\ cm^{-1}$	Cond	55.8	5	336
Total dissolved solids	$mg\ L^{-1}$	TDS	18.4	1.9	79.7
pH	-	pH	8.5	7.23	10
Depth	m	Depth	10.7	0.25	52
Total Nitrogen	$mg\ L^{-1}$	TN	0.3	0.01	3.4
Total Phosphorus	$mg\ L^{-1}$	TP	0.05	0	1.6
Sodium	$mg\ L^{-1}$	Na+	2.7	0.22	37.2
Potassium	$mg\ L^{-1}$	K+	0.5	0	4.5
Magnesium	$mg\ L^{-1}$	Mg^{2+}	2.2	0	20
Calcium	$mg\ L^{-1}$	Ca^{2+}	7.3	0.8	34.6
Chlorine	$mg\ L^{-1}$	Cl-	1.7	0	9
Sulfate	$mg\ L^{-1}$	SO42-	3.9	0.1	31.6
Loss-on-ignition	%	LOI	24.3	1.92	77.1

Table 2

		Axis 1	**Axis 2**	**Axis 3**	**Axis 4**
Eigenvalues		0.24	0.17	0.10	0.08
Cum % var. spp.		5.90	10.0	12.5	14.6
Cum% var. spp. - env. relation		33.5	57.0	71.2	82.7
Variable	**Total variance explained**	**Regression/canonical coefficeints**		**t-values of regression coefficients**	
	Axis 1	Axis 2		Axis 1	Axis 2
cond	4.4%	0.44	-0.27	3.99	-2.65
depth	2.0%	-0.15	-0.21	-1.90	-2.82
Na+	2.7%	0.10	0.02	0.91	-0.17
K+	4.8%	0.49	-0.07	4.67	-0.65
Cl-	3.4%	-0.21	0.65	-2.18	6.94
MJT	***4.4%***	***0.14***	***0.62***	***1.49***	***6.90***
LOI	3.1%	-0.09	0.04	-1.02	0.48

Table 3

Variable	**Covariable**	**% var. axis 1**	**% var. axis 2**	**p-value**	**λ1**	**λ2**	**λ1/λ2**
cond	none	4.40	7.90	0.001	0.179	0.317	0.560
	depth	4.60	7.90	0.001	0.181	0.315	0.570
	Na+	4.10	7.70	0.001	0.159	0.305	0.520
	K+	1.80	8.20	0.004	0.069	0.316	0.220
	Cl-	4.60	7.50	0.001	0.179	0.293	0.610
	MJT	3.60	8.10	0.001	0.140	0.313	0.450
	LOI	3.60	7.90	0.001	0.140	0.310	0.450
	ALL	1.70	7.60	0.016	0.057	0.259	0.220
depth	**none**	**2.00**	**9.80**	**0.001**	**0.082**	**0.397**	**0.210**
	cond	**2.20**	**8.10**	**0.002**	**0.083**	**0.315**	**0.260**
	Na+	**2.10**	**9.90**	**0.001**	**0.083**	**0.387**	**0.210**
	K+	**2.20**	**8.30**	**0.001**	**0.083**	**0.321**	**0.260**
	Cl-	**2.00**	**10.0**	**0.002**	**0.079**	**0.390**	**0.200**
	MJT	**2.00**	**9.60**	**0.001**	**0.077**	**0.371**	**0.210**
	LOI	**2.10**	**9.50**	**0.001**	**0.082**	**0.372**	**0.220**
	ALL	**2.20**	**7.60**	**0.001**	**0.074**	**0.259**	**0.290**
Na+	none	2.70	9.60	0.001	0.111	0.388	0.290
	Cond	2.40	7.80	0.001	0.091	0.305	0.300
	depth	2.80	9.80	0.001	0.112	0.387	0.290
	K+	2.30	7.70	0.001	0.089	0.296	0.300
	Cl-	2.70	8.90	0.001	0.106	0.347	0.310
	MJT	1.90	9.60	0.008	0.072	0.371	0.190
	LOI	2.40	9.60	0.001	0.093	0.375	0.250
	ALL	1.70	7.70	0.011	0.058	0.259	0.220
K+	**none**	**4.80**	**7.90**	**0.001**	**0.192**	**0.322**	**0.600**
	cond	**2.10**	**8.20**	**0.002**	**0.082**	**0.316**	**0.260**
	Na+	**4.30**	**7.60**	**0.001**	**0.171**	**0.296**	**0.580**
	Cl-	**5.00**	**7.40**	**0.001**	**0.195**	**0.290**	**0.670**
	LOI	**4.10**	**8.20**	**0.001**	**0.160**	**0.320**	**0.500**
	Depth	**4.90**	**8.10**	**0.001**	**0.193**	**0.321**	**0.600**
	MJT	**3.30**	**8.20**	**0.001**	**0.129**	**0.314**	**0.410**
	ALL	**2.00**	**7.70**	**0.003**	**0.069**	**0.259**	**0.270**
Cl-	**none**	**3.40**	**9.70**	**0.001**	**0.137**	**0.393**	**0.350**
	cond	**3.50**	**7.60**	**0.001**	**0.137**	**0.293**	**0.470**

	K+	**3.60**	**7.60**	**0.001**	**0.140**	**0.290**	**0.480**
	MJT	**3.20**	**8.60**	**0.001**	**0.125**	**0.332**	**0.380**
	LOI	**3.50**	**9.40**	**0.001**	**0.137**	**0.366**	**0.370**
	Depth	**3.40**	**9.90**	**0.001**	**0.134**	**0.390**	**0.340**
	Na+	**3.40**	**8.80**	**0.001**	**0.132**	**0.347**	**0.380**
	ALL	**2.80**	**7.60**	**0.001**	**0.098**	**0.259**	**0.380**
LOI	**none**	**3.10**	**9.30**	**0.001**	**0.124**	**0.377**	**0.330**
	Na+	**2.70**	**9.60**	**0.001**	**0.107**	**0.375**	**0.290**
	cond	**2.20**	**8.00**	**0.001**	**0.086**	**0.310**	**0.280**
	K+	**2.40**	**8.30**	**0.001**	**0.092**	**0.320**	**0.290**
	MJT	**3.00**	**9.30**	**0.001**	**0.116**	**0.361**	**0.320**
	Cl-	**3.20**	**9.40**	**0.001**	**0.124**	**0.366**	**0.340**
	Depth	**3.10**	**9.40**	**0.001**	**0.124**	**0.372**	**0.330**
	ALL	**2.20**	**7.60**	**0.001**	**0.074**	**0.259**	**0.290**
MJT	**none**	**4.40**	**9.10**	**0.001**	**0.176**	**0.371**	**0.470**
	Na+	**3.50**	**9.40**	**0.001**	**0.137**	**0.371**	**0.370**
	cond	**3.50**	**8.10**	**0.001**	**0.137**	**0.313**	**0.440**
	K+	**2.90**	**8.20**	**0.001**	**0.113**	**0.314**	**0.360**
	LOI	**4.30**	**9.20**	**0.001**	**0.168**	**0.361**	**0.470**
	Cl-	**4.20**	**8.50**	**0.001**	**0.164**	**0.332**	**0.490**
	Depth	**4.30**	**9.40**	**0.001**	**0.171**	**0.371**	**0.460**
	ALL	**2.70**	**7.50**	**0.001**	**0.091**	**0.259**	**0.350**

Table 4

a.

#	**Model type**	**Bootstrap R2**	**Bootstrap Average Bias**	**Bootstrap Maximum Bias**	**RMSE_s1**	**RMSE_s2**	**RMSEP**
1	**WA_Inv**	**0.61**	**0.06**	**5.30**	**0.69**	**2.19**	**2.30**
2	WA_Cla	0.61	0.07	4.78	0.86	2.20	2.36
Component 1	WA-PLS	0.60	0.02	5.28	0.71	2.22	2.33
Component 2	**WA-PLS**	**0.63**	**0.10**	**5.16**	**0.89**	**2.14**	**2.31**
Component 3	WA-PLS	0.60	0.07	5.08	1.03	2.19	2.41

b.

t-Test: Two-Sample Assuming Unequal Variances	***RMSEP of WA-PLS_C1***	***RMSEP of WA-PLS_C2***
Mean	0.0645	-0.0524
Variance	2.8822	1.5186
Observations	100	100
Hypothesized Mean Difference	0	
df	181	
t Stat	0.5570	
P(T<=t) one-tail	0.2891	
t Critical one-tail	2.3471	
P(T<=t) two-tail	0.5782	
t Critical two-tail	2.6033	
The P-Value is 0.01 < 0.05		**Reject null hypothesis**
The RMSEPs of WA-PLS C2 and WA-PLS C1 are different		